Additive Timber Jointing: Design and Robotic Manufacturing of Fiber-Aligned Mass Timber Connections

by
Ethan Frolov

A thesis accepted and approved in partial fulfillment of the
requirements for the degree of
Master of Science
in Architecture

Thesis Committee:
Dylan Wood, Chair
Cory Olsen, Member
Erica Fischer, Member

University of Oregon
Summer 2026

© 2026 Ethan Frolov
This work is openly licensed via CC BY 4.0.

THESIS ABSTRACT

Ethan Frolov

Master of Science in Architecture

Title: Additive Timber Jointing: Design and Robotic Manufacturing of Fiber-Aligned Mass Timber Connections

Mass timber construction has been increasingly dependent upon connections that are manufactured independently from the structural members they will eventually be joining. This typically requires significant structural material removal to fabricate CNC-machined interfaces in glue-laminated and cross-laminated timber, or reliance on sophisticated engineered metal hardware that isolates joinery from the manufacturing of structural members. This research proposes a design and manufacturing method for additively assembled timber joints in which fiber-aligned wood members are robotically placed to concentrate material and interconnection where structural demand is greatest, reducing reliance on subtractive machining while improving fabrication efficiency and structural performance.

Two joint typologies, a five-layer planar joint and a three-dimensional reciprocal joint, were designed through computational modeling and manufactured via robotic assembly to test this approach. Assembly reliability and fit were evaluated directly, while structural behavior is addressed qualitatively through comparison to a built all-wood precedent and a conceptual proposal for extending the same joint logic into a broader structural system. This work shows that a timber joint designed and fabricated with standard material can achieve greater continuity and simpler assembly than conventional connections, and that treating the joint as a primary design driver, rather than an afterthought to the structural member it connects, can reduce material use, manufacturing effort, and overall complexity.

ACKNOWLEDGMENTS

I am grateful to my thesis committee, Dylan Wood, Erica Fischer, and Cory Olsen, for their insightful feedback, genuine interest, and invaluable advice.

Special thanks to Dylan Wood and Judith Sheine, whose mentorship, guidance, and kindness were ever-present during the pursuit of this degree. Their commitment to advancing timber innovation has been, and continues to be, a wellspring of inspiration.

I would like to thank Nancy Cheng and Allison Kwok, both for introducing me to the world of Mass Timber and encouraging me to pursue what truly impassions me.

To my fellow MS students, Ri Zarate and Helene Brehl: I couldn't have asked for better friends and peers throughout this program. I cannot wait to see all the incredible things you will do.

Finally, thank you to my parents, Val and Denise Frolov, for their endless support and encouragement in my decision to pursue an even higher education. And to my girlfriend, Kayla: Thank you for your counsel, love, and patience throughout this foray, and every time else.

TABLE OF CONTENTS

THESIS ABSTRACT 3

ACKNOWLEDGMENTS 4

TABLE OF CONTENTS 5

LIST OF FIGURES 7

CHAPTER I INTRODUCTION 9

1.1 Motivation 9

1.2 Opportunity 10

1.3 Research Questions 10

1.4 Organization of Thesis 11

CHAPTER II BACKGROUND 12

2.1 Historical and Contemporary Timber Joinery 12

2.2 Engineered Wood and Mass Timber Systems 13

2.3 Digital Fabrication in Timber Construction 14

2.4 Robotic Assembly and Discrete-Element Timber Systems 16

2.5 Additive vs. Subtractive Approaches to Joint Formation 17

2.6 Environmental Considerations and the Benefits of Mass Timber 17

2.7 State of the Art 18

2.8 Identified Gaps in Current Research 19

CHAPTER III SCOPE 20

3.1 Focus 20

CHAPTER IV METHODOLOGY 21

4.1 General Methodology 21

4.2 Computational Design to Manufacturing Workflows 22

4.3 Physical Prototyping 23

4.4 Testing and Evaluation Procedures....25
4.5 Evaluation Scope....26
CHAPTER V RESULTS....28
5.1 Exploratory Design Phase....28
5.2 Part 1: Design and Prototyping of a Planar Joint....31
5.3 Structural Comparison with the Heartwood Building....35
5.4 Part 2: Design and Prototyping of a 3D Joint....40
5.5 Design Concept....43
CHAPTER VI DISCUSSION....48
6.1 Fabrication Performance Across Both Prototypes....48
CHAPTER VII CONCLUSION....49
7.1 Summary....49
7.2 Limitations and Future Work....50
7.3 Impact....51
REFERENCES CITED....54

LIST OF FIGURES

Figure 1. Simplified schematic diagram of interlocking wood grain formed at a bifurcation. 9

Figure 2. Traditional Dougong compared to a modern digital reinterpretation in the form of a discretized Dougong voxel. 12

Figure 3. Digital fabrication of a modular timber frame structure using clip joints. 15

Figure 4. Control sensors on a gripper used to train reinforcement learning models in robotically assembled double-lap joints. 16

Figure 5. Philip J. Currie Dinosaur Museum, multi-layered joint, assembled additively. 18

Figure 6. Real-world precedent joints: Heartwood, Tamedia Office Building, and the Fisher & Paykel Appliances Global Headquarters. 18

Figure 7. Outline of general methodology. 21

Figure 8. Pick-and-place motion sequence for a single layer of the planar joint. 23

Figure 9. The fully assembled planar joint and three-dimensional multi-axis joint. 24

Figure 10. Photographs showing the basic process of forming a prototype additive wood joint. 26

Figure 11. Photographs, axonometric diagrams, and exploded axonometric views of early exploratory joint studies. 28

Figure 12. Diagrammatic sequence of the non-orthogonal interlock joint design exploration. 29

Figure 13. Visual explanation of DRMM's "Knuckle Joint" and its wedge variation. 29

Figure 14. Diagrammatic build sequence of the gradient density joint. 30

Figure 15. The Clad Planar joint, from concept to assembly. 32

Figure 16. The clad planar joint repeated across a structural grid. 33

Figure 17. The UR20's fixed working envelope. 34

Figure 18. Build sequence of the first layer of the clad planar joint. 34

Figure 19. Moment diagram for a typical fixed beam-column connection compared with the joint's rigid-arm connector. 36

Figure 20. Smoke and superheated air path of travel at Heartwood's beam-to-column connection. .39

Figure 21. Smoke and superheated air path of travel at the planar joint's beam-to-column connection.....40

Figure 22. The completed three-dimensional multi-axis joint, viewed from above.....41

Figure 23. Partial build sequence of the first layer of the multi-axis joint.....42

Figure 24. Material-grade distribution for the three-dimensional multi-axis joint.....44

Figure 25. Force distribution diagram for the 3D joint's beam-column intersection.....46

Figure 26. Cross-sectional proportioning at the three-dimensional multi-axis joint, informed by the force distribution shown in Figure 25.....47

Figure 27. Build sequence for a single reciprocal frame arrangement of four joints.....47

CHAPTER I
INTRODUCTION

1.1 Motivation

Timber construction has long depended on a subtractive logic: structural connections are shaped by removing material, cutting, milling, or carving a joint out of a larger piece of wood until the desired geometry remains. Contemporary mass timber construction continues this tradition, forming connections either through CNC machining, which mills material away from an engineered wood member, or through prefabricated metal hardware attached after the member is made. Both treat the joint as something produced after the fact, a separate operation performed downstream of the process that formed the wood itself [1].

This separation carries real costs, and they become harder to ignore as mass timber construction scales into larger, more complex buildings. Material removed during machining is material that once contributed to the member's overall strength. Metal hardware exists less because wood itself is weak, and more because achieving reliable, high-precision all-wood joinery at scale has been difficult. In the world of Mass Timber, steel fills a precision gap, not a strength gap. Moreover, connection fabrication is detached from member fabrication, meaning opportunities to design the two in collaboration are lost before the work even begins.

An alternative is possible. Rather than carving a joint out of a finished member, a joint can be built up; formed by robotically assembling many small components into a larger composite connection. This additive approach treats the joint not as something subtracted after the fact, but as something constructed alongside the member, woven into the process that forms the wood. Much

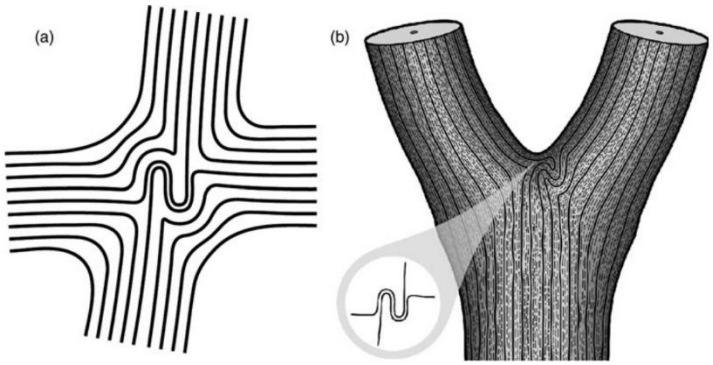


Figure 1. Simplified schematic diagram of interlocking wood grain formed at a bifurcation.

as a tree grows its grain organically along the paths that carry structural forces most efficiently (Figure 1A & 1B) [2], these small wood elements can be oriented with intention rather than inheriting the grain direction of sawn lumber.

1.2 Opportunity

This shift opens more than an efficiency gain. If a joint is built up rather than carved away, the placement of each small element becomes a design decision, one that can respond to where a connection needs strength rather than to the boundaries a milling tool happens to leave behind. Robotic assembly makes this kind of control practical at a useful scale, placing many small components with a consistency and repeatability that hand assembly cannot match, unconstrained by the fixed tool geometry that limits what a mill can cut [3, 4].

Mass timber practice has been slow to take advantage of this shift. Robotic fabrication in timber construction is still used almost exclusively to automate subtractive processes, cutting and drilling faster and more precisely, rather than to build connections up from smaller parts [5, 3]. The opportunity this research pursues is not only a new joint typology, but a change in what robotic fabrication is asked to do: not so much an automated mill, but rather more an assembler of many small, deliberately placed pieces, each contributing to a connection's strength, material efficiency, and structural behavior in ways a single machined block cannot.

1.3 Research Questions

These opportunities lead to a broader question: how can robotic fabrication be extended beyond machining, into the direct construction of a joint's structural logic? This thesis targets wood-to-wood joints built from small or standard members, robotically assembled and oriented to respond to anticipated force paths rather than to the fixed geometry a milling tool leaves behind. While this focus area spans structural design, robotic fabrication, and material behavior, the approach of this thesis is to develop and demonstrate an integrated process. Ideally, one that could be extended and refined within each of those disciplines individually. From this context, the following research questions are developed:

1. How can the intentional alignment and assembly of small or standard wood members along anticipated force paths enhance the strength-to-mass ratio and structural performance of wood-to-wood joints?

2. What robotic assembly strategies and additive manufacturing sequences can most effectively construct fiber-aligned wood joints while minimizing assembly time and alignment errors?
3. How can a combined analysis of strength-to-mass ratio, assembly time, and material use reveal useful tradeoffs in the design of digitally fabricated, additive timber joints?

Within these questions, the project focuses first on design-manufacturing integration, then on structural performance, and finally on fabrication efficiency. The reasoning behind each joint's alignment logic is developed further in later chapters.

1.4 Organization of Thesis

This thesis is organized into seven chapters. Chapter 1 introduces motivation, opportunity, and research questions guiding the work. Chapter 2 reviews background literature on timber joinery, engineered wood systems, digital and robotic fabrication, and additive versus subtractive approaches to joint formation. Chapter 3 defines the scope and focus of the research. Chapter 4 presents the methodology, including computational modeling, physical prototyping, and testing and evaluation procedures. Chapter 5 reports the results of the exploratory design phase, the design and prototyping of the planar and three-dimensional joints, a structural and fire-performance comparison with the Heartwood building, and each joint's broader design-concept potential. Chapter 6 compares fabrication performance across both prototypes. Chapter 7 concludes with a summary, limitations and future work, and the broader impact of the research.

CHAPTER II
BACKGROUND

2.1 Historical and Contemporary Timber Joinery

Traditional timber joinery achieved structural connections entirely through geometry, without adhesives or metal fasteners. Japanese Tugite and Shiguchi joints, for example, comprise roughly 200 documented variants generated by combining a small set of basic interlocking shapes, each suited to a specific structural function such as resisting gravity or resisting pull-apart forces [6]. Chinese Dougong bracket systems achieve similar ends through layered, interlocking timber components assembled without fasteners, a joinery logic recently reinterpreted through robotic fabrication research, visualized in Figure 2 [7]. These traditions demonstrate that geometry alone, carefully considered, can carry substantial structural demand, a principle that remains relevant even as fabrication methods have changed. Contemporary mechanical testing supports this principle: an evaluation of self-locking, interlocking furniture-frame joints confirmed meaningful strength and stiffness from geometry alone, without adhesives or metal fasteners [8].

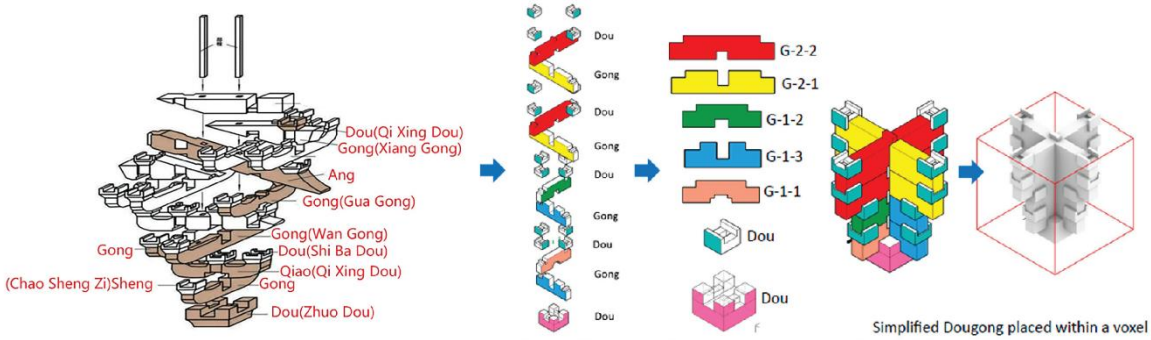


Figure 2. Traditional Dougong compared to a modern digital reinterpretation in the form of a discretized Dougong voxel.

Contemporary mass timber systems, by contrast, rely heavily on engineered products such as glulam and CLT, most often connected using metal fasteners or CNC-machined interfaces rather than the interlocking geometries of traditional joinery [9, 1]. Subtractive machining removes significant material, demands extensive production time, and isolates connection fabrication from the manufacturing of structural members. As mass timber applications grow in scale and complexity, the disconnect between traditional joinery logic and modern production workflows becomes more pronounced.

Recent research demonstrates the potential of digitally fabricated wood-wood connections to achieve higher performance with less waste. CNC-produced interlocking joints made from LVL panels have been shown to exceed EC5 strength predictions by up to 25 percent in shear and compression, though the result is not universal: joints made from OSB panels underperformed EC5's prediction by roughly the same margin, indicating that panel material, not joint geometry alone, governs how closely a digitally produced connection follows code prediction [10, 11]. A synthesis of historical and contemporary joinery illuminates expected behavior across typologies, while a related study connects joinery geometry to embodied carbon outcomes, reinforcing the sustainability benefits of all-wood connections [12, 13]. Efforts to digitally reproduce traditional joinery, translating Tugite and Shiguchi patterns into CNC-milled and 3D-printed forms, or reinterpreting Dougong assemblies for robotic construction, further illustrate how historical joinery logic continues to inform contemporary digital fabrication [6, 7].

2.2 Engineered Wood and Mass Timber Systems

Mass timber construction is built from a handful of standardized engineered wood products, chief among them glue-laminated timber, cross-laminated timber, and mass plywood panels, each of which extends the structural capacity of dimensional lumber or veneer by bonding smaller elements into large, standardized components. These products have driven mass timber's rapid adoption across North America and Europe as a lower-carbon alternative to steel and concrete, and they form the material substrate that any timber joint, additive or subtractive, ultimately must connect to. Yet the connections between these engineered elements are treated much in the same way this thesis has already described joints in general: formed downstream, after the member itself is manufactured, most often through metal fasteners, adhesives, or CNC-machined interfaces. That dependency has motivated a growing body of research into adhesive- and metal-free assembly techniques [9]. That same downstream, subtractive logic is worth investigating as to how and why these engineered products are manufactured the way they are in the first place.

One such approach relies on wood's own moisture-driven swelling rather than a fastener at all. A dry dowel, inserted into a pre-drilled hole in lamellae carrying a higher moisture content, swells as it re-equilibrates with ambient humidity and locks the joint through friction alone [9]. Plain wood dowels loosen over time, since the dowel shrinks as the hole expands with dropping humidity, but densified wood dowels resist that decline through a lingering set-recovery tendency left over from the densification process, which keeps them swelled against the hole long after installation and lets a

dowel be cut smaller than its hole for easier, more robotic-friendly insertion. The technique demonstrates that a fully wood, fastener-free connection can stay durable over time, and it is one of the clearer precedents for the dowel-based future work discussed in Chapter 7.

The tension between subtractive and additive logic is not unique to joint design. It appears throughout the manufacturing of engineered wood products themselves. Cross-laminated timber, for instance, layers finger-jointed lumber in alternating orthogonal directions, cross-stacking and adhesive-pressing those layers, only reaching its final geometry through CNC trimming and edge-profiling, a subtractive step applied after the panel's core material has already been formed [14]. Dowel-laminated timber offers a partial counterpoint: softwood lamellas are joined with friction-fit hardwood dowels rather than adhesive, making it the only widely produced mass timber product that is entirely wood, without adhesives or metal fasteners [14]. These manufacturing choices matter beyond the panel itself. Mass timber's appeal rests significantly on speed and weight - completed buildings are typically 40 to 50 percent lighter than equivalent concrete structures, and construction schedules average roughly 3 to 4 days per story compared to about 28 days per story for reinforced concrete [14]. Manufacturing decisions that add material efficiency or shave production steps, at the panel scale or the joint scale, compound directly into those advantages.

Waste follows a similar pattern. Non-hazardous waste from CLT production runs to roughly 97.6 kilograms per cubic meter of product, nearly three times the 32.4 kilograms per cubic meter generated by glued laminated timber, driven largely by the finger-jointing and planing required for glulam's long, defect-free laminations and by its tighter moisture-control tolerances relative to CLT [15]. That figure also excludes waste from CNC detailing and edge-trimming, the final cutting and profiling each member undergoes after panel manufacture, which is less significant for glulam's simpler rectangular sections than for CLT's more complex trimmed geometry, but remains notable regardless, since the ends of nearly every member are trimmed or cut away. If inefficiency at this scale persists in how the panels themselves are manufactured, it raises the question of how much waste accumulates at the connection scale, where, unlike panel production, there is comparatively little published data. That gap is where this thesis positions its own contribution.

2.3 Digital Fabrication in Timber Construction

Digital fabrication has begun to answer that question, at least in part, though not by discarding subtractive methods so much as by asking what robotics can add that CNC machining alone cannot. This shift can be framed precisely: conventional automation in timber construction focuses on

processing individual parts, while robotic timber construction reframes fabrication around the assembly of many generic members in space, placing material exactly where it is needed rather than milling it away from stock that already exists in its final form [16]. That reframing, from processing single parts to assembling many of them, is close to the logic this thesis pursues at the scale of a single joint.

Other research has approached the same question from the direction of translation rather than reinvention. One study digitally analyzed and reparametrized traditional Japanese wood joints for CNC fabrication, documenting accuracy improvements over manual methods [6], while another reviewed robotic technologies applied to reinterpreting historical Dougong-style multi-layer timber joints with contemporary tools [7]. A more experimental approach integrated 3D-printed clip joints with timber framing in a modular, reversible connection system that abandons machined wood-to-wood contact altogether as seen in Figure 3 [17]. A related approach applies the same printed-node logic to bamboo, scanning each pole's individual geometry to customize a 3D-printed connector informed by structural analysis, extending printed-intermediary joinery to a naturally variable, unmilled material [28]. Each demonstrates a different relationship between digital tools and joinery, translating an existing form, reinterpreting a historical one, or replacing timber-to-timber contact with a printed intermediary, but all point toward the same conclusion: digital fabrication expands what is structurally and geometrically possible in timber joinery well beyond what subtractive machining alone can achieve.



Figure 3. Digital fabrication of a modular timber frame structure using clip joints: Digital node design (left), node 3D printing (left middle), CNC milled timber plywood bars (middle), hand assembly (right middle), and final assembly (right).

2.4 Robotic Assembly and Discrete-Element Timber Systems

Robotic assembly extends this expansion further by allowing structures to be built from many discrete elements rather than shaped as a whole. Reinforcement-learning-based robotic strategies have been developed to manage friction, alignment, and contact uncertainty during timber assembly, capacities directly relevant to additive workflows using many small components [5].

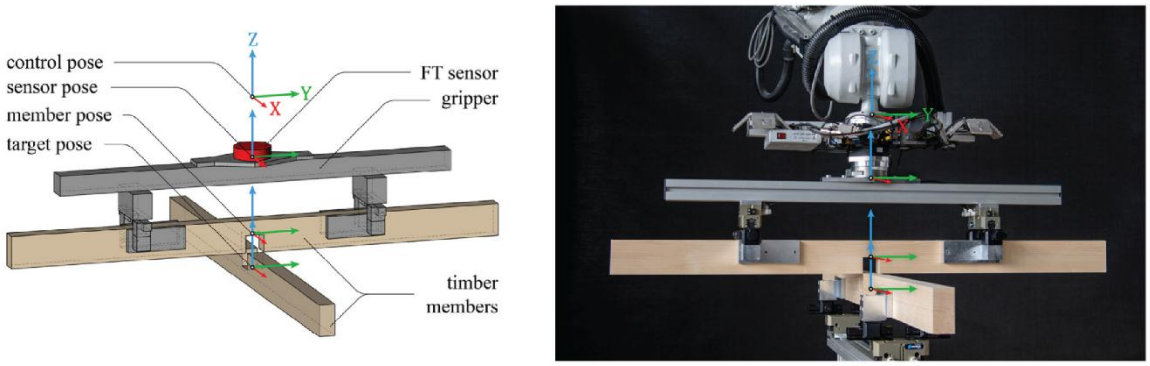


Figure 4. Control sensors on a gripper used to train reinforcement learning models in building robotically assembled double-lap joints.

This trajectory advances further through modular, discrete-element beam construction using robotic assembly and digital twins, demonstrating how voxelized or element-based design can align with automated production and reliably aggregate small timber units into larger structural components with high precision [3]. The same uncertainty problem has also been approached from a different angle, using a digital twin and Learning by Demonstration to robotically assemble timber trusses joined by three-dimensional interlocking cross-lap joints, with a force-compliance controller that lets the robot adapt to small positioning errors and manufacturing imperfections in real time rather than requiring a perfectly precise setup [18]. Where these studies focus on the mechanics of placing individual pieces, other work addresses what happens once they are placed: a design framework linking parametric modeling of free-form timber plate structures with finite element analysis, explicitly accounting for semi-rigid wood-wood connections, offers a computational template for understanding how local joint stiffness influences global structural behavior [19]. Together, these lines of work, robust placement under uncertainty, aggregation of many small elements, and modeling the connections those elements form, describe much of what an additive, robotically assembled joint requires to function structurally.

At the scale of a full building system, TRIQBRIQ demonstrates a related discrete-element strategy: small, robotically manufactured timber blocks stacked and interlocked with wood dowels

on site, entirely without adhesives or metal fasteners, and designed to be disassembled and reused by type [29]. Spatial Timber Assembly takes the inverse approach, using cooperating robotic arms to fabricate and position whole timber beams directly into complex, non-orthogonal spatial frames, achieving geometric complexity through assembly logic rather than the piecewise composition of many small elements [30].

2.5 Additive vs. Subtractive Approaches to Joint Formation

Across historical joinery, engineered wood, digital fabrication, and robotic assembly, one pattern holds regardless of tool or era: the joint is almost always formed by removing material after the fact. Hand-cut Tugite and Shiguchi joints, CNC-milled connections, and robotically assembled discrete-element structures alike still typically arrive at their final geometry by cutting into a piece of wood, whether by hand, mill, or arm, along a plane chosen for fit rather than for how the wood's grain runs through it. Grain orientation in that piece is fixed by the tree it came from. A skilled hand, or a CNC operator manually adjusting a toolpath, can choose where to cut relative to that grain, but neither can reassign the grain itself once the piece is set. Additive assembly changes what is available to work with in the first place, because the joint is built from many small, individually placed members rather than carved from one. Grain orientation then becomes an independently assignable property of each piece rather than an inherited constraint of a single component.

2.6 Environmental Considerations and the Benefits of Mass Timber

Mass timber's environmental case rests on a mechanism concrete and steel cannot replicate: trees remove roughly two tonnes of CO2 from the atmosphere for every tonne of dry wood they form, and that carbon stays locked in the material for as long as the building stands rather than being released back into the atmosphere. The effect is measurable at building scale. Brock Commons Tallwood House, an 18-story mass timber high-rise at the University of British Columbia, stores an estimated 1,753 tonnes of CO2 in its wood structure and avoided 679 tonnes of greenhouse gas emissions relative to a concrete equivalent, savings comparable to taking 510 cars off the road for a year [14]. A review of this and similar projects against conventional construction concludes that mass timber outperforms concrete and steel across most of the criteria that matter for material selection, not only carbon but water use and onsite waste as well [14].

That case depends on how the timber is actually joined. Most engineered wood products are assembled with synthetic adhesives or metal fasteners, and both carry a cost the base material does not: glue-laminated timber embodies roughly 60% more energy than sawn timber, and although adhesive typically makes up only about 1.4% of a cross-laminated timber panel's mass, it accounts for around 31% of that panel's global warming potential and total energy impact, and 57% of its eutrophication potential [9]. Adhesives and metal fasteners also complicate the reuse and recycling of timber at end of life, can off-gas volatile organic compounds during service, and are consistently the first component to fail in a fire, since the timber itself chars and retains strength long after a glue line or steel plate has given way. Mass timber's sequestered carbon only stays sequestered if the building it is part of has a long service life, and connections that resist reuse or fail early work against that goal.

2.7 State of the Art

Built projects provide complementary insight into real-world mass timber performance and connection logic. The Philip J. Currie Dinosaur Museum by Teeple Architects and StructureCraft showcases advanced engineered wood geometries assembled with high-precision digital fabrication,



Figure 5. Philip J. Currie Dinosaur Museum, multi-layered joint, assembled additively. A: Finished and installed joint. B: Hand assembly process C: The joint in elevation view.

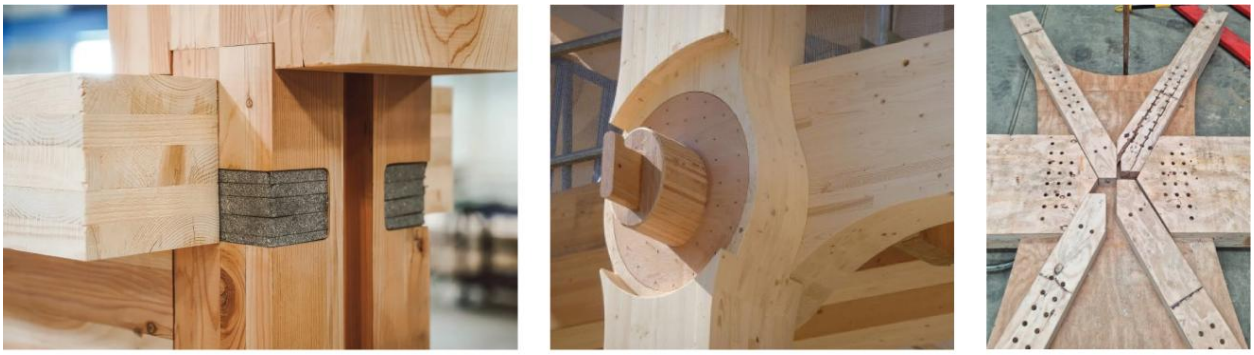


Figure 6. From left to right: A). Heartwood - Mortise & tenon joint B). Tamedia Office Building – Peg and dowel joint C). The Fisher & Paykel Appliances Global Headquarters – Timber diagrid Joint.

demonstrating how alternative approaches to building up joint connections layer by layer can form atypical joint typologies (Figure 5) [20]. Heartwood by atelierjones presents a rare North American example of mass timber construction that prioritizes wood joinery over conventional metal hardware (Figure 6A) [22]. Shigeru Ban and Hermann Blumer's Tamedia Office Building demonstrates the structural and architectural power of all-wood joinery at scale, using meticulously fabricated connections that avoid steel fasteners but still depend heavily on subtractive processes (Figure 6B) [21]. A related precedent comes from a design study for a timber diagrid seismic structural system: an engineered-wood diagrid built from repeated, connection-driven geometry, with particular attention to connection ductility under demanding loading (Figure 6C) [23]. That system's non-orthogonal, angled node geometry was an early reference point while scoping this thesis's own angled joint typology, though that typology was ultimately deferred to future work rather than developed here. These projects illustrate the promise of mass timber but also reinforce limitations that arise when connection manufacturing remains separated from material production and constrained by subtractive workflows.

2.8 Identified Gaps in Current Research

Taken together, these bodies of work point to a consistent absence rather than a single unresolved question. Timber joinery, whether hand-cut or CNC-milled, still treats the joint as something subtracted from a finished member after the fact, and engineered wood manufacturing does not currently integrate joint formation into the lamination process itself, leaving connection design and material production as separate operations [1]. Digital fabrication and robotic assembly have demonstrated real capability for managing many small, discretely placed elements with precision, and recent work has begun optimizing joint geometry computationally within otherwise conventional fabrication workflows [24], but none of this capability has been directed specifically at forming joints from fiber-aligned, additively assembled components. Fiber orientation itself is rarely treated as a variable available to the designer at all: interlocking, oriented-grain assemblies remain studied mostly in natural forms rather than engineered ones [2].

This project addresses these gaps by examining additive joint formation through robotic assembly, positioning this strategy as a pathway toward more efficient, materially responsible, and high-performance mass timber connections.

CHAPTER III
SCOPE

3.1 Focus

This research proposes that additive strategies for forming timber joints, built through robotically assembled small-element configurations, make fiber orientation an assignable design parameter rather than a fixed property inherited from a single piece of stock. Aligning grain along anticipated force paths at the point of assembly, rather than working around whatever orientation a subtractively formed joint happens to retain, is expected to improve structural performance while reducing reliance on subtractive machining. This expectation rests on robotic assembly's ability to position and orient individual members with a consistency manual methods struggle to match. Moving away from metal connectors toward all-wood joinery also reduces the embodied carbon tied to fastener and hardware production, and the efficiency gained from aligning fiber with anticipated force paths allows narrower beams and columns to carry the same load, lowering overall material demand. The same logic extends to material selection: sections of a member that see less load could use lower-grade species or offcut material, putting stock to use that would otherwise be wasted.

Additive timber joinery is examined as a robotic assembly process, in which small members are aggregated to form composite joints that are then attached to or integrated with larger structural elements.

This research focuses on two robotically assembled joint typologies: a clad planar joint, a five-layer, 104-piece planar assembly formed from robotically placed components, and a three-dimensional multi-axis reciprocal joint that extends the same additive logic across three orthogonal axes. Together, these two typologies are sufficient to demonstrate the fabrication process and the geometric logic behind it. A third typology, a robotically assembled angled joint, is discussed in Chapter 7 as a direction for future work, one example among many possible extensions of this approach beyond strictly orthogonal configurations.

CHAPTER IV
METHODOLOGY

4.1 General Methodology

The process follows a consistent pipeline across both joint typologies. Design intent, grounded in fiber-aligned, force-path geometry, is translated into a parametric joint model built in Rhino and Grasshopper, which generates joint typologies, layering patterns, and assembly logic. From this model, robotic toolpaths are generated and executed as robotic assembly, producing a physical

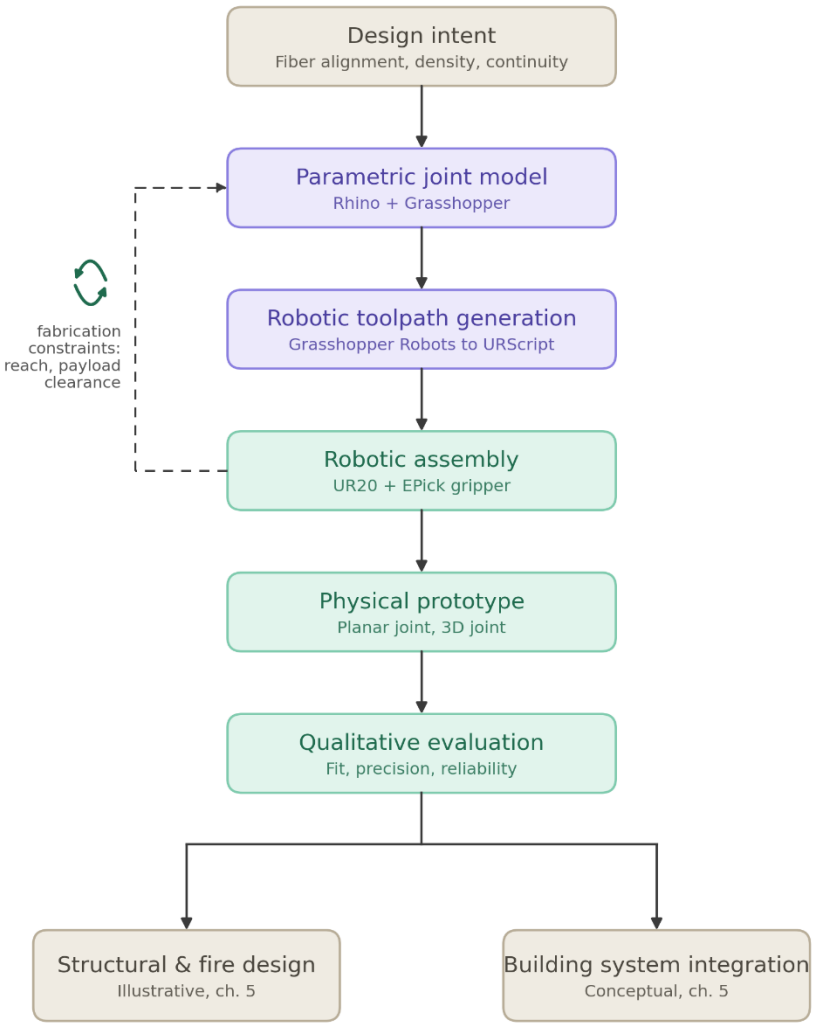


Figure 7. Outline of general methodology

prototype. Each prototype is then evaluated qualitatively for fit, precision, and assembly reliability (Section 4.4). Fabrication constraints encountered during assembly, principally the UR20's reach, payload, and clearance limits, were fed back into the parametric model to adjust parameters such as member dimensions, approach vectors, or pathing. Findings from this cycle inform two downstream discussions, an illustrative structural and fire design argument and a conceptual extension toward building system integration, both developed in Chapter 5.

4.2 Computational Design to Manufacturing Workflows

Computational modeling supports generating joint geometries, designing robotic toolpaths, and simulating assembly sequences. Rhino and Grasshopper are used to create parametric models of joint typologies, enabling fast iteration on layering patterns, member orientations, and assembly logic. Robotic toolpaths and assembly sequences are developed using Grasshopper-based robotics plugins and simulation environments to test feasibility prior to physical trials, informed by research on tolerance-aware and adaptive robotic timber assembly [5].

Robotic toolpaths and assembly sequences are developed in Grasshopper using the Robots plugin, which generates URScript output for execution on the physical robot through Polyscope (v5.21.1), the UR control software. Parametric models define pickup and placement targets, board dimension offsets, and axis-selectable rotations for each component, allowing rapid iteration on layering patterns and assembly sequencing before physical trials. Motion speed and blend zone are controlled at runtime through Custom Command nodes that reassign shared speed and zone variables, allowing slow, precise motion during pickup and placement and faster transit motion elsewhere without maintaining separate per-target speed lists. Stress-trajectory analysis, originally proposed as a basis for fiber-aligned geometry generation, was not carried forward into the final workflow.

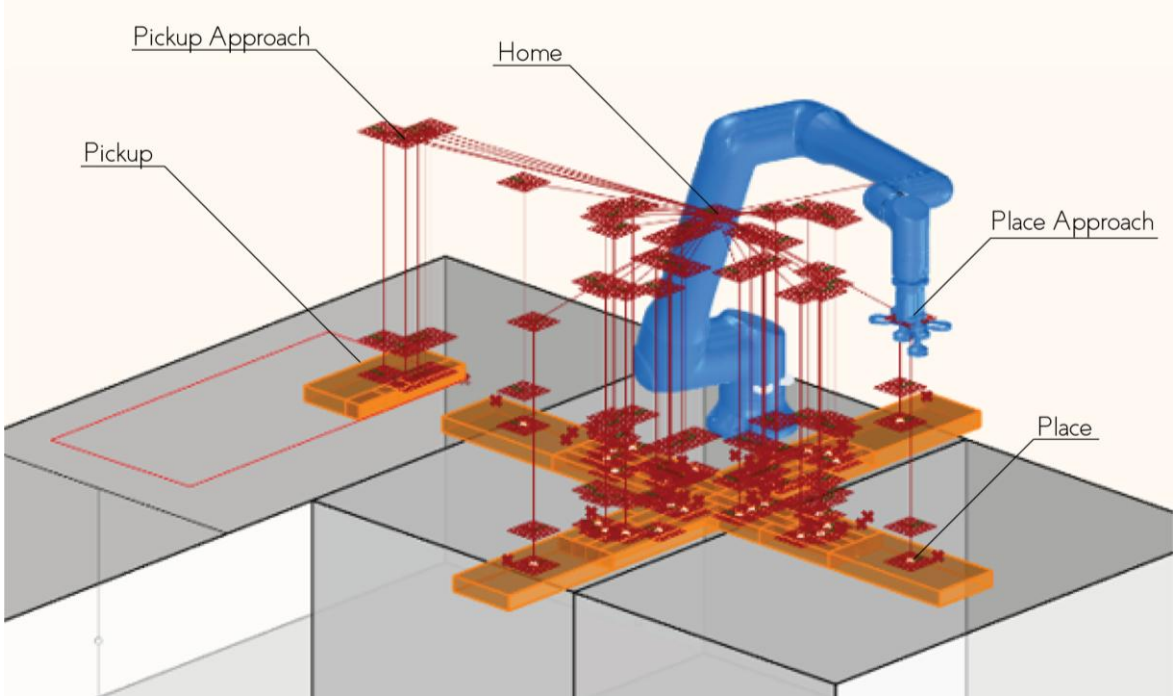


Figure 8. Pick-and-place motion sequence for a single layer of the planar joint, labeled by motion phase: pickup, pickup approach, home, place approach, and place.

4.3 Physical Prototyping

The research makes use of a robotic arm, wood gluing equipment, and a fully equipped woodshop. The experimental strategy uses an initial exploratory phase followed by a focused comparative phase. In the exploratory phase as discussed later in 5.1, a larger set of potential additive joints is modeled and prototyped at small scale to understand basic behavior, fabrication feasibility, and assembly logic. From this set, joint typologies are selected for deeper study, with physical samples fabricated to allow comparison and observation of consistency. Prototypes focus on the joint region and immediate surrounding material rather than full structural elements. Robotically assembled joints are built from smaller, discrete members that are then attached to or integrated with larger members.

Material selection followed two tracks. The physical prototypes built for this thesis each used a single species: the planar joint was fabricated in yellow poplar, and the three-dimensional multi-axis joint in Douglas fir, both seen in Figure 9. Single-species construction was a deliberate choice given the absence of structural testing at this stage, since the individual contributions of different species in a multi-material scheme would be buried within the joint and therefore impossible to verify

without load testing. The built prototypes were treated instead as a test of whether robotically assisted assembly could achieve complex, geometrically demanding joinery at all, rather than as a proof of multi-species structural optimization. The wood species chosen themselves, yellow poplar and Douglas fir, were chosen on the basis of cost and local availability.

Beyond these built prototypes, material selection was also considered as a distribution problem within a single joint, and this idea should be read as a driver of the joint's form and application, not merely an unrealized detail. Structural input from Erica Fischer suggested that the core of a beam-scale assembly carries comparatively little stress, while the corners and outer members, particularly those participating directly in moment-resisting behavior, carry substantially more.

This points toward a design logic in which a combination of common hardwoods and softwoods native to Oregon, where mass timber production for this project is based, could be allocated by location: stronger species reserved for zones carrying concentrated compressive or tensile demand, and weaker or offcut species used as infill where demand is lower, with the species mix tunable to meet structural standards, adjusted for local availability, or varied by use case and use location if this process were adapted elsewhere. This stratification logic shapes both the internal composition of a joint and the broader adaptability of the approach across regions and applications.



Figure 9. The fully assembled planar joint made with yellow poplar (left) and the fully assembled three-dimensional multi-axis joint made with Douglas fir (right).

It was considered during design but was not physically fabricated or tested at this scale within this thesis; validating it under structural load is identified as a direction for future work.

Robotic assembly is performed with a UR20 six-axis robotic arm fitted with a Robotiq EPick vacuum gripper, programmed through Grasshopper's Robots plugin and executed via URScript on Polyscope. Each pickup-and-placement sequence follows a consistent program structure: home position, approach, pre-pickup, pickup with vacuum grip engaged, retract, return to home, quadrant-based approach to the placement location, approach-to-place, place, nudge to seat the component and compress the suction cup, release, retreat, and return to home. Placement geometry is defined parametrically, with axis-selectable rotation and diagonal offset moves computed as vector combinations of the local board axes. Boards requiring a shoulder-flipped robot configuration are run as separate program batches rather than switched mid-sequence, since the configuration change requires open space and deliberate testing. When individual board sequences are merged into a single program, a fixed joint-angle move is injected at each board-boundary home position to prevent the robot from inheriting the prior board's ending configuration and faulting on axis limits.

4.4 Testing and Evaluation Procedures

Evaluation of each prototype was primarily qualitative rather than instrumented. The central questions were practical: did the robot place components reliably and repeatably as programmed, could the same process be adapted to different joint geometries and piece shapes, and were the resulting joints assembled to a reasonable degree of quality and speed. The answer to each was yes. A substantial share of the development effort went into programming pickup and placement targets precisely enough that each hand-milled piece would seat correctly on approach, since even small angular or positional errors could prevent a piece from fitting where it needed to go. Once that calibration was in place, the robot's advantage became clear: it removes much of the difficulty traditionally associated with assembling small, complex components, since a person only needs to sequence the pieces correctly and provide a fixation method, glue, dowels, screws, or similar, while the robot holds each piece in place until instructed that it has been secured.

The main limiting factor observed was not the robot's placement precision but the precision of the hand-milled components themselves. Each piece used to construct the joints was milled by hand, and while this produced pieces of adequate quality to assemble the joints successfully, minor cumulative tolerance errors and small inconsistencies between pieces, attributable to the limits of hand tools and eye measurement rather than the robotic process, were observed. This suggests that

fabricating the discrete elements with a CNC mill or laser cutter, where the geometry allows, or simply by a more skilled craftsperson, would likely improve both consistency and assembly speed beyond what was achieved here.

Fixation during glue-up was also evaluated for drift. Early small-scale prototypes were clamped using a vacuum press, and a minor degree of drift occurred during curing, consistent with a concern raised during committee review that vacuum-press glue-up on loosely fitted joints could shift pieces out of alignment and require post-glueup milling to correct. Larger-scale prototypes were clamped conventionally rather than with a vacuum press, since their size exceeded what the available vacuum equipment could accommodate, and did not exhibit this drift issue.

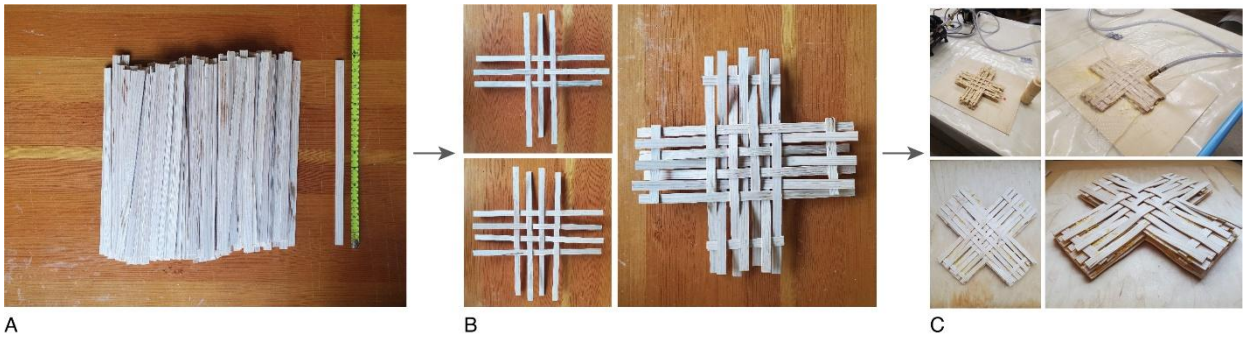


Figure 10. Photographs read left to right, showing the basic process of forming a prototype additive wood joint. A: Wood fiber milled and processed. B: Wood fibers aligned to the desired final arrangement for one layer. C: Layers glued, stacked, and placed in a vacuum press for between 6 – 12 hours.

4.5 Evaluation Scope

This thesis evaluates whether a fully wood, additively assembled joint can outperform conventional CNC-cut wood-wood connections across the metrics that matter most for mass timber design: strength-to-mass ratio, ease and speed of assembly, and material efficiency. Two joint typologies were designed and fabricated to test this directly. The planar joint is a five-layer, 104-piece assembly; the three-dimensional joint totals sixty-six pieces. Both are built from individually placed members, each adaptable in species, dimension, and position to the structural demand at its specific location, rather than fixed by whatever a single piece of milled stock allows. Mass is known directly, from the piece counts and calculated weights of each build. Strength is addressed analytically rather than through physical load testing, using the rigid-end-zone argument developed in Chapter 5. This shows, illustratively, how a rigid, moment-resisting wood joint, achieved through geometric analysis

and precise fiber placement, reduces the bending moment a connecting beam must resist, allowing that beam to carry its load with less material. Together, these results show that adaptable, additively assembled wood joints can be designed, fabricated, and installed with relative ease. Chapter 5 also shows conceptually how the same joint logic can extend into a building system to reduce material demand and ease assembly. While a full embodied carbon assessment is beyond the scope of this study, material efficiency and potential reduction of waste are noted in future work.

CHAPTER V

RESULTS

5.1 Exploratory Design Phase

The exploratory phase began with simple material studies rather than structural claims. Early cross-laminated joints used thin Douglas fir lamella strips (Figure 11A), then rotated plywood layer (Figure 11B), before finally moving to solid Douglas fir boards (Figures 11C & D). Each iteration alternated grain direction between layers to maintain overlap and test how small discrete members behave once aggregated: how density built up, where the assembly wanted to hold together, and where it wanted to pull apart. What became clear almost immediately was that the orientation of

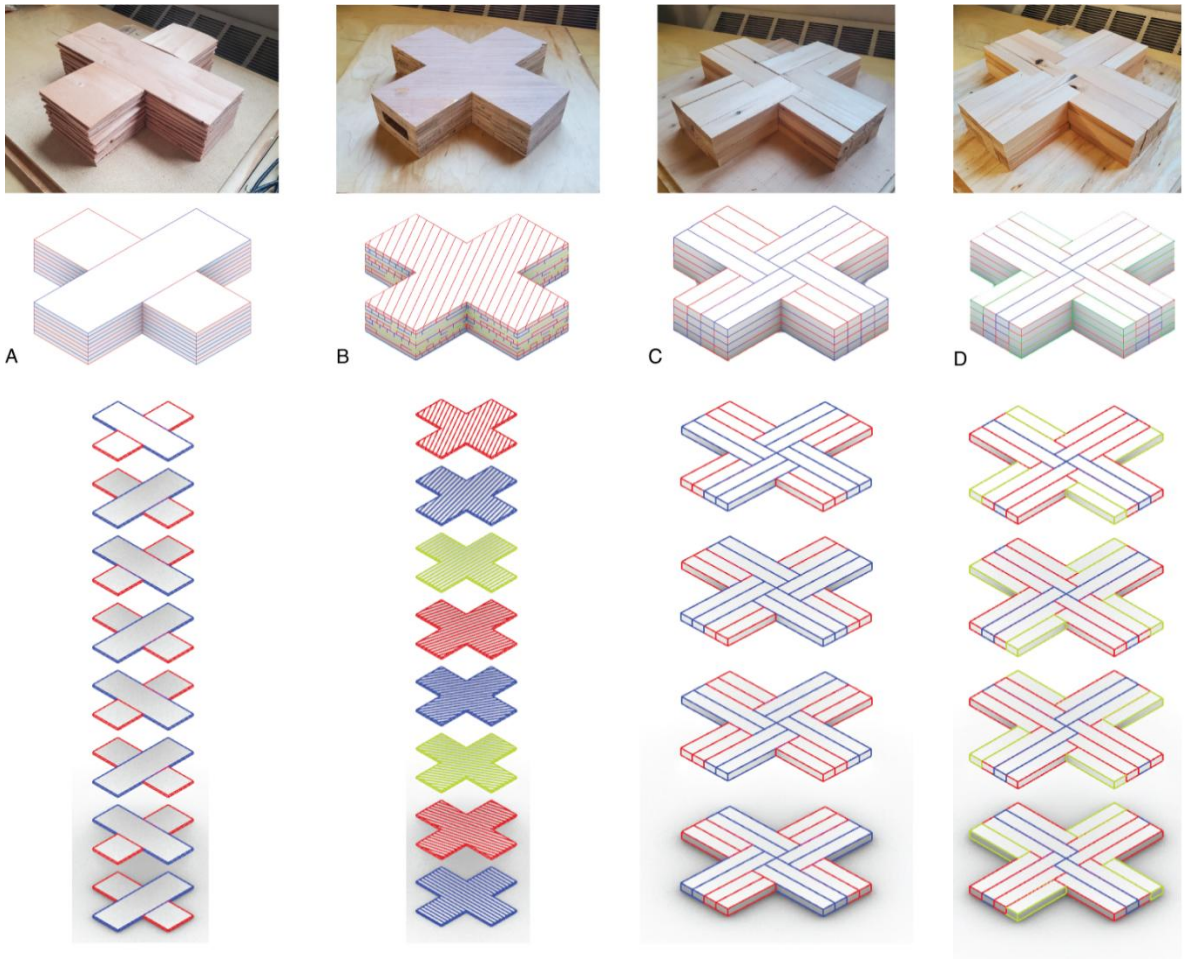


Figure 11. Photographs, axonometric diagrams, and exploded axonometric views of early exploratory joint studies. A. Cross-laminated thin Douglas fir lamella strips. B: Cross-laminated plywood, each layer rotated 45 degrees. C. Double interlocking solid Douglas fir boards. D: Triple interlock solid Douglas fir boards. The bottom row depicts each configuration exploded along its layering axis, colored by individual member to denote size or rotation.

each member, relative to its neighbors and to the direction of load, mattered enormously. That observation carried directly into the next step: interlocking boards, first with two unique unit sizes, then three, each configuration relying on a reciprocal push, every piece bearing against the ones around it under tension or compression, so that the joint had no single point of failure and grew stronger as more of it came together.

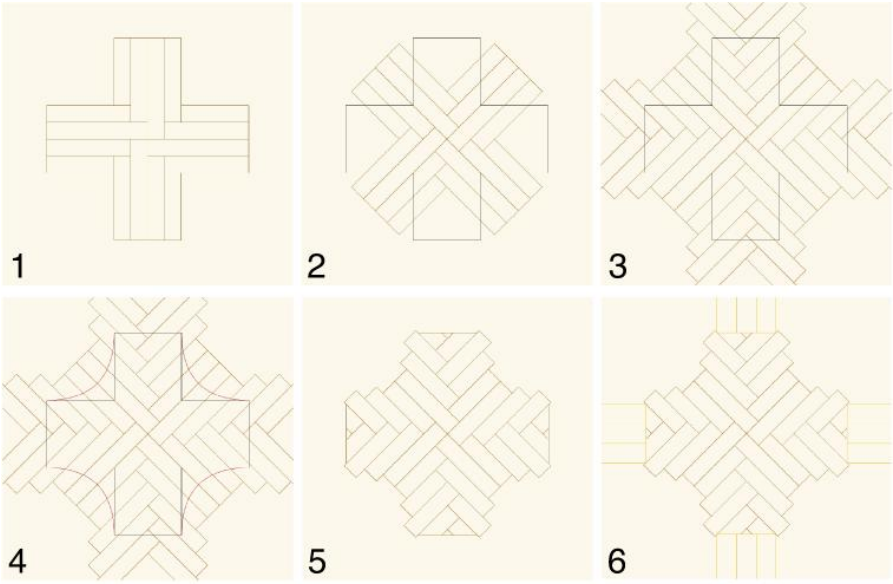


Figure 12. Diagrammatic sequence of the non-orthogonal interlock joint design exploration in a sectional view, read left to right, top to bottom.

That insight led directly to the interlocking wedge joint, explored across several variants: a non-orthogonal interlock joint, several keyhole geometries, and a hardwood-core version. The wedge geometry was inspired by dRMM's Knuckle Joint, a hardwood CLT connection developed through the Building from Forests research project, which uses a tapered hardwood knuckle to transfer force at a post-and-beam interface without metal flitch plates or bolts [25]. That precedent's wedge, placed exactly where force wanted to travel rather than where a milling tool made cutting convenient, was a

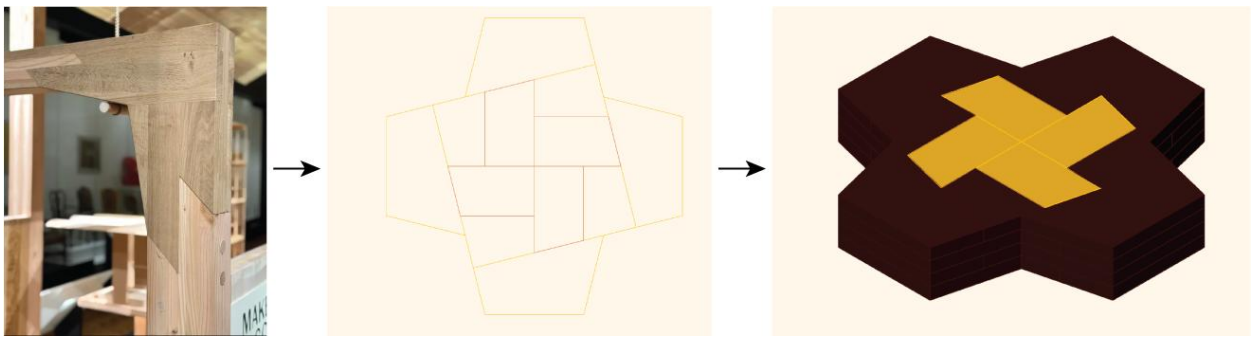


Figure 13. dRMM's "Knuckle Joint" [25] (left) inspired a wedge variation of the interlocking joint. Center: plan diagram of the wedge geometry. Right: the resulting joint, with a softwood core clad in a hardwood exterior.

direct model for testing whether a softwood core wrapped in a hardwood exterior could achieve a similar effect within an additively assembled joint, an early version of the wood fiber material distribution logic later applied to the planar and 3D joints.

That interlocking logic led to a more significant development: the gradient density joint. In any joint under load, stress does not distribute evenly, it concentrates at bearing surfaces, along shear planes, and at corners where geometry changes. A CNC-milled joint cannot respond to that unevenness, since subtractive machining removes material uniformly across the whole connection. An additively assembled joint can: member density was varied across the connection, denser where forces concentrated, sparser where they did not, based on where the geometry of the joint itself suggested force was concentrating. That shift, from a joint with uniform material distribution to one where density responds directly to anticipated demand, shaped the design logic that followed. This logic extended further into how these small members could interleave with the lay-up of a larger component, such as a glulam column, so that the discrete elements forming the connection became continuous with the discrete elements forming the member itself.

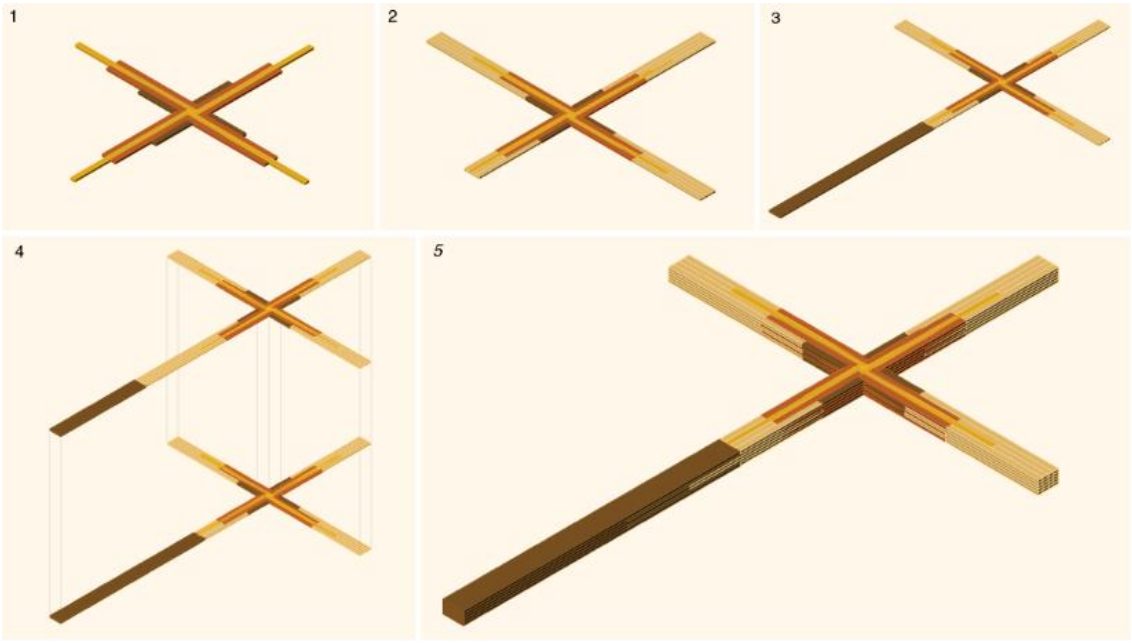


Figure 14. Diagrammatic build sequence of the gradient density joint, read left to right and top to bottom. 1-3: Member proportions and orientations are varied to test how density can shift across the connection. 4: Layers are stacked and offset to build density through the joint's depth. 5: The assembled joint, showing the resulting density gradient across its cross-section. Note: Colors in this diagram are meant for visual clarity of different component sizes, not necessarily different materials.

The final design step of the exploratory phase extended this logic into three dimensions. Everything built up to that point had been essentially planar, operating in two axes, but a real beam-to-column connection must resolve force in three. The multidirectional joint applied reciprocal frame logic, members mutually supporting each other in a continuous rotational arrangement with no single primary member, to a configuration of discrete elements interlocking along all three axes. Male and female connectors were added to the ends of these nodes to test what a repeatable, modular grid of such connections might look like, each joint becoming a module, each module capable of linking to the next. This directly foreshadowed the three-dimensional multi-axis joint developed later.

5.2 Part 1: Design and Prototyping of a Planar Joint

These threads converged in the clad planar joint developed across the rest of this chapter. The same density gradient explored above carries through to the final iteration directly. At the joint's center, where the four members cross and the geometry is most complex, the assembly is built from smaller, more numerous pieces; moving outward along each arm, the pieces grow larger and the layout simplifies. The joint's outer layer of members forms a cladding condition, an exterior sheath that sandwiches the interior pieces together and gives the joint a finished outer surface. In the built prototype that cladding logic is carried by geometry and piece layout alone, not by a second species: since Part 1 was not subjected to structural testing or a built application that required the distinction. The entire joint, core and cladding alike, was fabricated in the single yellow poplar species discussed in Chapter 4, preserving the design logic without the material contrast it was originally conceived around.



Figure 15. The Clad Planar joint, from concept to assembly. A: Exploded axonometric sequence showing the hardwood cladding (dark) and softwood core (light) coming together layer by layer. B: Assembled isometric view, color-coded to distinguish the hardwood cladding wrapping the softwood core. C: The clad planar joint under robotic assembly. Built in a single yellow poplar species, the cladding logic is carried through the geometry rather than material contrast.

Part 1, the clad planar joint, is complete: a five-layer, 104-piece robotically assembled connection, built in yellow poplar following the single-species rationale discussed in Chapter 4. Ten distinct piece types make up the assembly, each with its own calculated mass, so the robot's payload setting changed continuously throughout the run to match whichever piece was currently being placed, and each piece's pickup and placement orientation was set individually, since not every piece sits the same way within its layer.

The joint's overall scale was set largely by the UR20's working envelope rather than by structural ambition. With a 1750 mm reach, every pickup and placement point had to fall within an area small enough that the complete joint could be assembled without repositioning the robot, which placed a hard ceiling on how large any single typology could grow. Carrying capacity, by contrast, was never a limiting factor: piece weights, calculated from the yellow poplar's measured density, ranged from roughly 0.63 lb for the smallest unit to about 11.4 lb for the largest, both well under the arm's 20 kg standard payload. The more immediate constraint was the gripper itself. Its 41 mm suction cups required a minimum board width of about 2 inches to seat reliably, which set a practical lower bound on how narrow any individual piece could be.

To situate the joint beyond the scale of a single prototype, the completed connection was also modeled in context as a single four-way column-beam intersection, repeated across a full structural grid mockup. Because this connection type recurs at nearly every column-beam intersection in a typical timber frame, these renders demonstrate that the density-and-overlap strategy developed for Part 1 applies broadly across a structure, not only to one isolated joint condition.

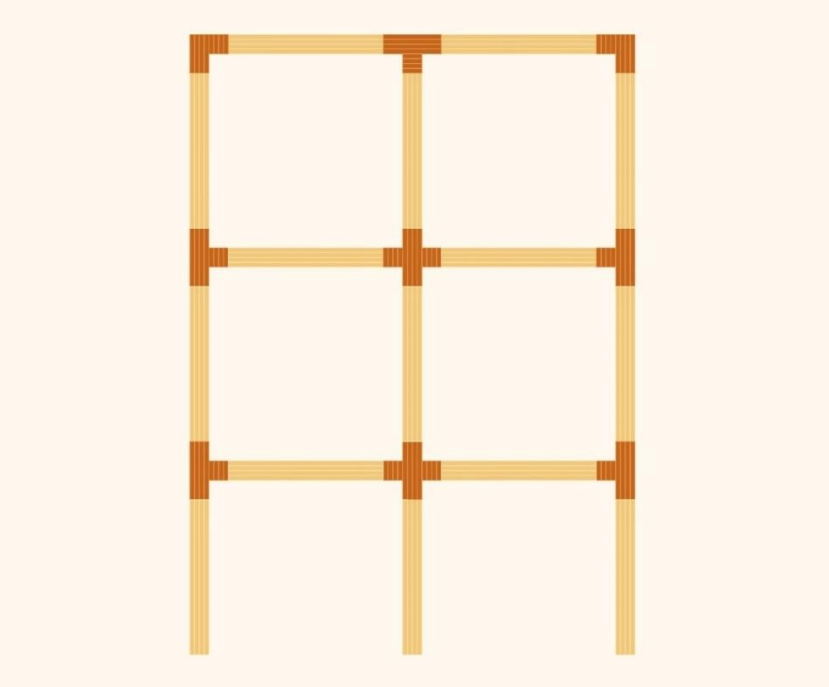


Figure 16. The clad planar joint repeated across a structural grid, abstracted to a bounded 2x2 bay fragment to represent the connection's recurrence across a larger timber frame.

Part 1's central challenge was keeping several parallel data streams, motion targets, gripper commands, and per-piece payload values, aligned to the same build sequence. Nearly every early fault traced back to misaligned or misindexed data rather than any physical hardware problem: payload values pulled from the wrong lookup structure produced scrambled masses, and a data-entry error shuffled part of one layer's build order, a mistake that then propagated into its mirrored layer.

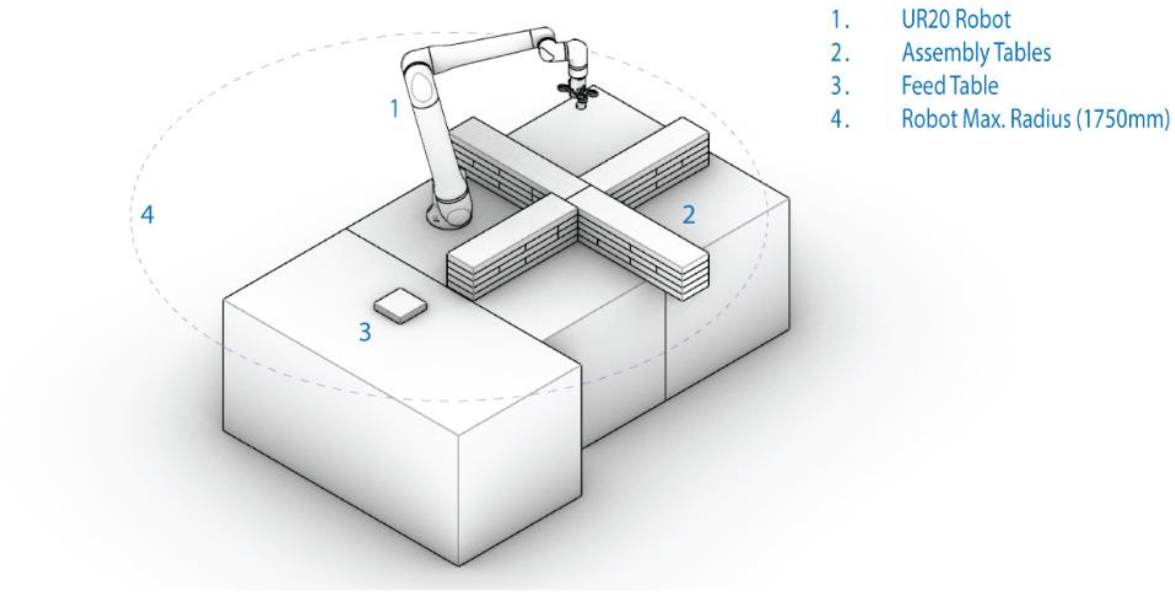


Figure 17. The UR20's fixed working envelope. Assembly tables, a feed table, and a 1750 mm maximum reach radius set the practical footprint within which every pickup and placement had to occur.

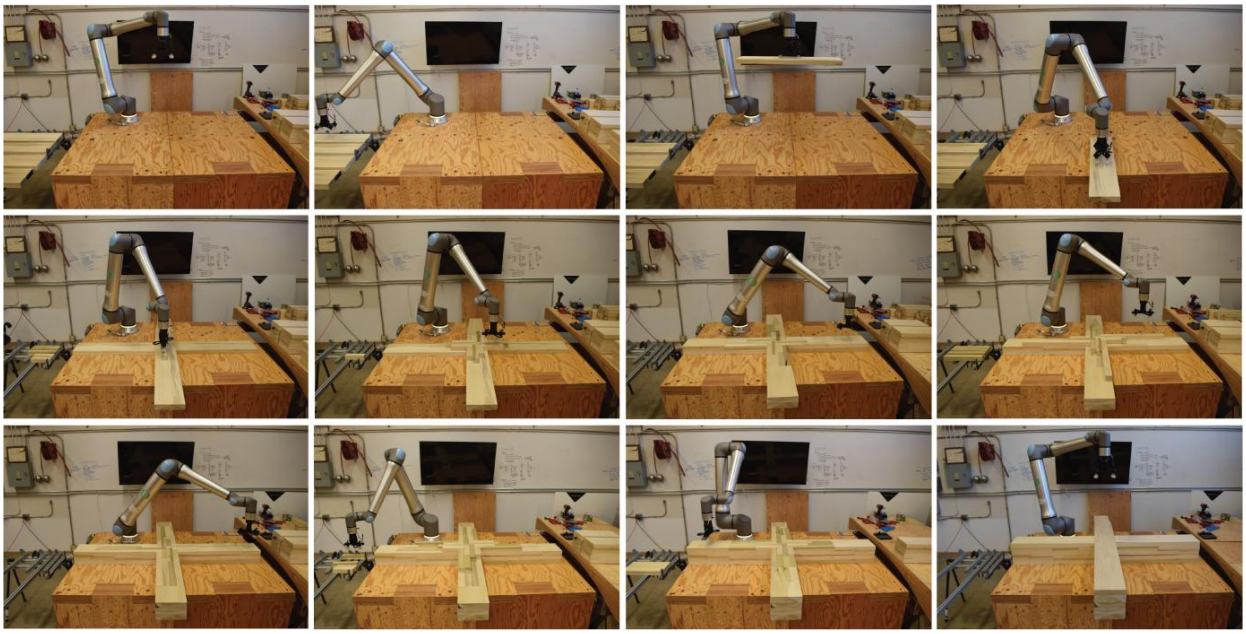


Figure 18. Build sequence of the first layer of the clad planar joint and the start of the second. Read from left to right, top to bottom.

A vacuum gripper that fired but wouldn't hold pieces looked at first like a hardware fault, but a control test on the gripper itself proved the seal and suction were fine, isolating the real cause to a line in the script that shut the vacuum back off if it didn't confirm fast enough. Diagnosing these issues correctly, rather than assuming the robot or gripper was at fault, meant a repeatable command-injection pipeline could be built once and reused across every layer.

5.3 Structural Comparison with the Heartwood Building

Heartwood, the all-wood connection system introduced in Chapter 2, offers a useful structural point of comparison for the planar joint [22]. Heartwood's beam-to-column connections are idealized structurally as pins, transferring shear and bearing stress but no moment, so even though the column itself runs continuously through the wall behind it, the load only ever has one route down through a single line of contact. This is consistent with how the connection is actually detailed. What matters structurally at that joint is having enough bearing area, not resisting a bending moment, because by definition, none reaches it.

That simplicity at the connection is not free, though. Because the pin refuses to share any moment with the column, the full bending demand has to be carried by the beam alone, and it concentrates at midspan rather than at the support. Idealized as a simply supported beam under a uniform load w over a span L, the moment along its length is $M(x) = wx(L - x)/2$, zero at each pin and maximum at midspan, $M(L/2) = wL^2/8$. That midspan value is the largest of any condition considered here: a connection that takes on no moment itself simply passes the entire burden to the beam, unassisted. By contrast, a connection that shares even a modest amount of that moment, the naive fixed case introduced next, cuts the beam's midspan demand to a third of Heartwood's, $wL^2/24$ versus $wL^2/8$, before any rigid-arm extension is added at all.

A rigid, moment-resisting connection changes this picture entirely. Where Heartwood's pin asks nothing of the connection itself beyond adequate bearing, leaving the beam to carry its full midspan moment alone, a connection stiff enough to resist rotation shares that burden instead, letting a designer choose where along the beam's length the bending moment peaks, and, more importantly, where it does not. The planar joint's four rigid arms are built for exactly this purpose: because each arm is substantially stiffer than the timber beam it connects to, the arm can reasonably be idealized, following standard structural practice for stiffened beam-column joints, as a rigid end zone, a region the beam effectively does not see as part of its flexible span. Extending that rigid zone further out

from the column face pushes the effective span the beam must bend across, and with it the connection's demand for material, correspondingly lower.

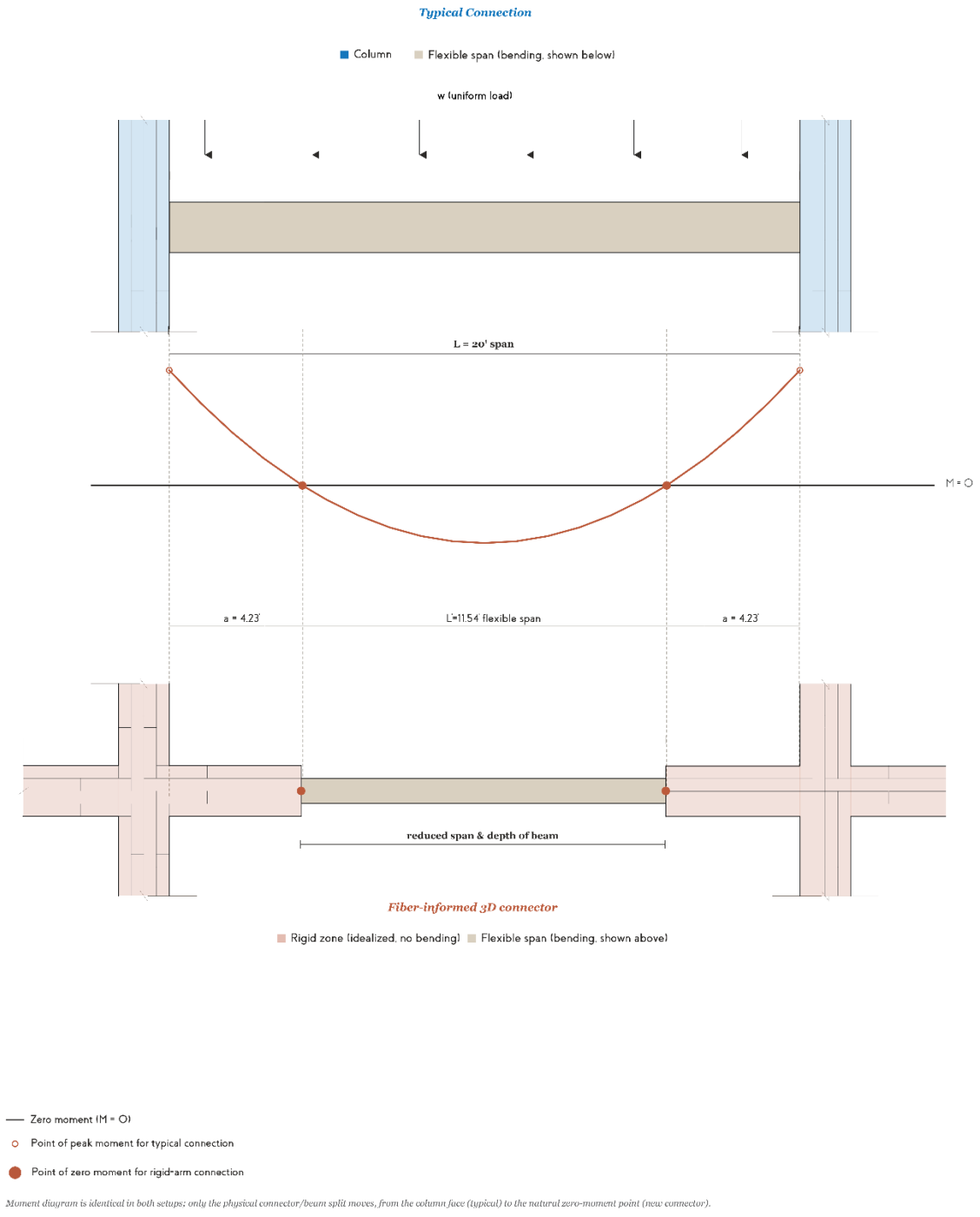


Figure 19. Moment diagram for a typical fixed beam-column connection (top) compared with the joint's fiber-informed rigid-arm connector (bottom), sharing a single moment diagram. The typical connection hogs $wL^2/12$ at the column

Consider first the naive case: a beam of length L fixed against rotation at both ends and carrying a uniform load w, the standard idealization for a beam framing rigidly into two columns with no rigid extension at the connection. Fixed-fixed beam theory gives the moment along the span as $M(x) = wLx/2 - wx^2/2 - wL^2/12$, producing a hogging moment of $wL^2/12$ at each support and a sagging moment of half that, $wL^2/24$, at midspan. Non-dimensionalizing with $t = x/L$ and solving $M(t) = 0$ places the moment's zero crossing at $t = (3 - \sqrt{3})/6$, approximately 0.2113 of the span in from each support, a coefficient that comes directly from the quadratic and is permanently irrational, the same way π is fixed in a circle. For an illustrative span of L = 20 ft, chosen only to demonstrate the method and not a measured design value, the moment at the column face is taken here as the 100 percent reference case, and the zero crossing falls 4.23 ft in from the column (Figure 19, top).

The joint's rigid arms exploit this same diagram directly, rather than producing a new one. Because the moment already crosses zero 4.23 ft in from each column face, extending each rigid arm exactly that far lets the beam's own flexible span begin and end right where the moment is already zero. The arm absorbs the entire hogging region nearest the column, the portion of the diagram a conventional beam would otherwise have to resist at $wL^2/12$, while the beam itself only ever sees the reduced middle segment, $L' = L - 2(4.23 \text{ ft}) \approx 11.54$ ft for this illustrative span, where the moment never exceeds the sagging value at midspan, $wL^2/24$ (Figure 19, bottom).

The comparison, then, is between the two peak values on that single diagram. A conventional beam framing rigidly into the column has to be sized for the larger of the two, the hogging moment at the column face, $wL^2/12$. Because the arm has already absorbed that region, the beam behind this joint only has to be sized for the smaller value, the sagging moment at midspan, $wL^2/24$, exactly half. The zero-crossing point itself never moves; it was always sitting 4.23 ft in from the column face, whether or not anything physically ended there. What changes is where the connector actually places the beam's boundary, at that already-existing zero-moment point rather than at the column face itself.

That reduction matters because bending moment, not shear or axial load, typically governs a timber beam's required depth for a given allowable stress and span. A beam designed to resist half the moment can be shallower, and a shallower beam is both lighter and requires less fiber overall, considerations that compound directly into lower material cost and easier handling and installation on site, both of which matter more in mass timber construction than in steel or concrete, where crane capacity and per-piece weight already constrain constructability. Extending the connection's rigid lever arm, in other words, is not only a structural refinement; it is a design lever that trades a

small amount of additional material at the joint itself for potentially much larger material savings across the length of the beam it connects to.

This idea, sizing a connection's rigid offset to intentionally relocate a beam's moment demand, is well established in steel and reinforced concrete design, where rigid end-zone or rigid-offset modeling is standard practice in structural analysis software for stiffened beam-column joints. Applied to an all-wood connection, it has not been meaningfully explored. Conventional timber connections, bolted plates, steel brackets, or milled notches, do not typically offer a rigid, extended arm of the kind this joint's dense, fiber-aligned core provides; timber's comparatively low stiffness and the difficulty of creating a truly rigid all-wood transition have generally kept this lever-arm strategy out of wood construction. The planar joint's additively assembled, density-graded core is what makes the idealization defensible in the first place: concentrating shorter, more numerous, higher-density members near the connection is precisely what gives the arm the stiffness the rigid end-zone assumption requires.

These figures are illustrative and load-independent, expressed as a ratio and a fraction of span so that no particular load case or member size is being claimed. The rigid end-zone idealization itself depends on the arm actually being substantially stiffer than the beam, an assumption that is standard practice for the general method but has not yet been confirmed against the planar joint's actual built dimensions and species modulus of elasticity. Comparable all-wood beam-column connections using compressed wood connectors have been physically tested for moment-rotation behavior elsewhere, suggesting this kind of validation is achievable for this joint as well [26]. Confirming it here would mean comparing the arm's effective stiffness to the beam's using Part 1's real fabricated geometry, work identified in section 7.2 as a direction for future study.

A closely related precedent exists in reinforced concrete design. Conventional reinforcement typically follows a uniform orthogonal grid regardless of local demand, but recent digital methods trace rebar layouts along a structure's principal stress directions instead, concentrating steel where tensile forces are highest and thinning it out elsewhere. This approach has been applied to a flat slab and a folded shell, tracing rebar to follow computed stress flow rather than a fixed grid, and the resulting layouts required up to 32 percent less steel than a conventional orthogonal grid while carrying the same load [27]. The underlying logic, grading a reinforcing material's density and placement to match localized structural demand rather than distributing it uniformly, parallels this thesis's own approach to species and member placement within a joint: higher-value or stiffer wood allocated to regions under greater tension or compression, with lower-grade material filling zones

that carry comparatively little load. Where reinforced concrete achieves this by tracing steel along computed stress trajectories, this thesis pursues the same principle through the discrete, additively assembled placement of individual wood members, each one positioned according to anticipated force demand rather than the constraints of a single milled piece.

Heartwood's pinned, subtractive detailing carries a second consequence worth noting, independent of moment behavior. Heartwood's beam sits in a notch milled into the column, and the floor slab rests on top of the beam in turn, so every interface in that assembly is a resting connection rather than a continuous one, each with its own small fabrication tolerance gap. Traced through the full assembly, these gaps line up into a continuous vertical path between floors, effectively a chimney for oxygen and fire to travel along the connection line. The real Heartwood building appears to treat this as a known condition: it uses intumescent tape specifically at these floor-to-floor connections, a fire-stopping measure that would not be necessary if the gaps did not actually align.

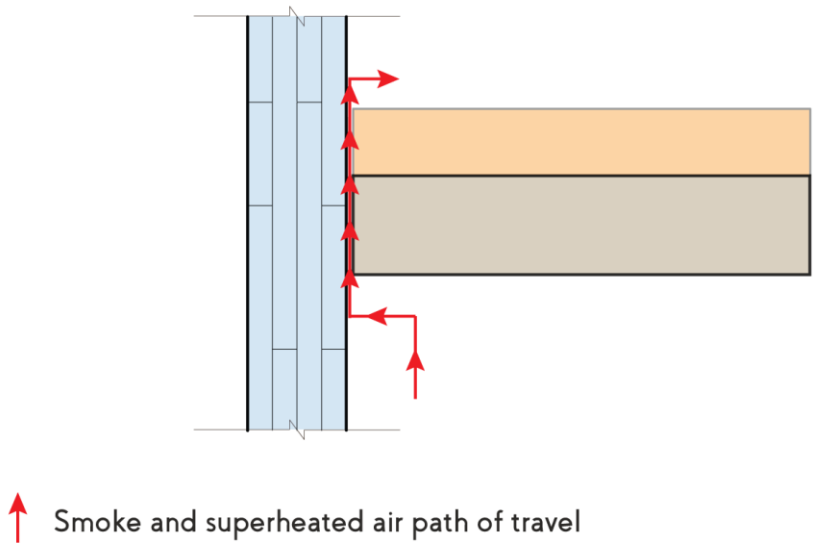


Figure 20. Smoke and superheated air path of travel at Heartwood's beam-to-column connection. The beam's milled notch and the floor slab's resting bearing above it are each independent interfaces with their own fabrication tolerance gap, and those gaps align into a continuous vertical path between floors.

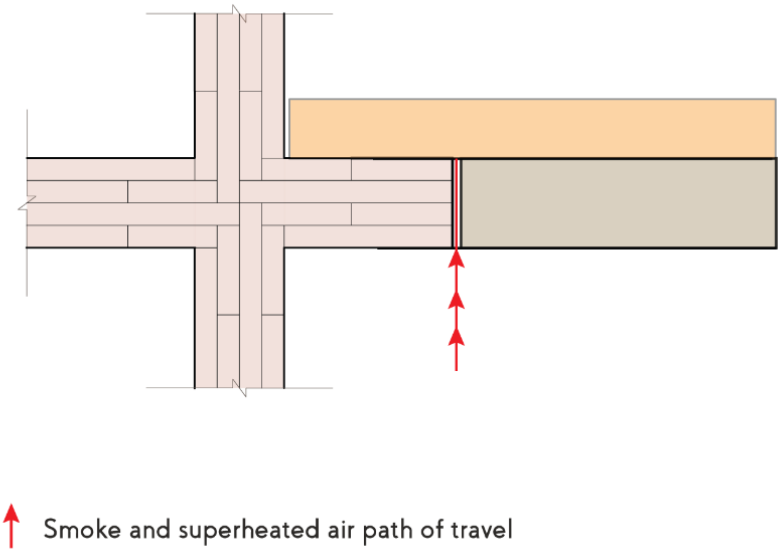


Figure 21. Smoke and superheated air path of travel at the planar joint's beam-to-column connection. The arm's staggered, layered geometry carries the floor slab across a broad, continuous bearing surface, so no fabrication tolerance gap has an aligned path to travel through.

The planar joint's extended arm geometry offers a related, though independent, advantage here as well. Because the arm extends the connection outward from the core, the floor slab can bear on the arm's broad, continuous surface rather than a single small notch, so no gap has an obvious path to line up into a continuous channel the way Heartwood's does. This is a defensible geometric claim, that the staggered, layered arrangement leaves no aligned gap line, not a claim that no gap exists at all; fabrication always leaves some tolerance, and confirming this advantage fully would require building and inspecting the actual connection.

5.4 Part 2: Design and Prototyping of a 3D Joint

The three-dimensional joint pushed this further still: suction strength and travel speed could be adjusted mid-sequence, and the robot's placement zone, its positional tolerance at each waypoint, could be tightened or disabled outright wherever a piece needed to land with precision rather than blend smoothly into the next move. What began as an unfamiliar and challenging process became, with each iteration, a more legible and controllable one.

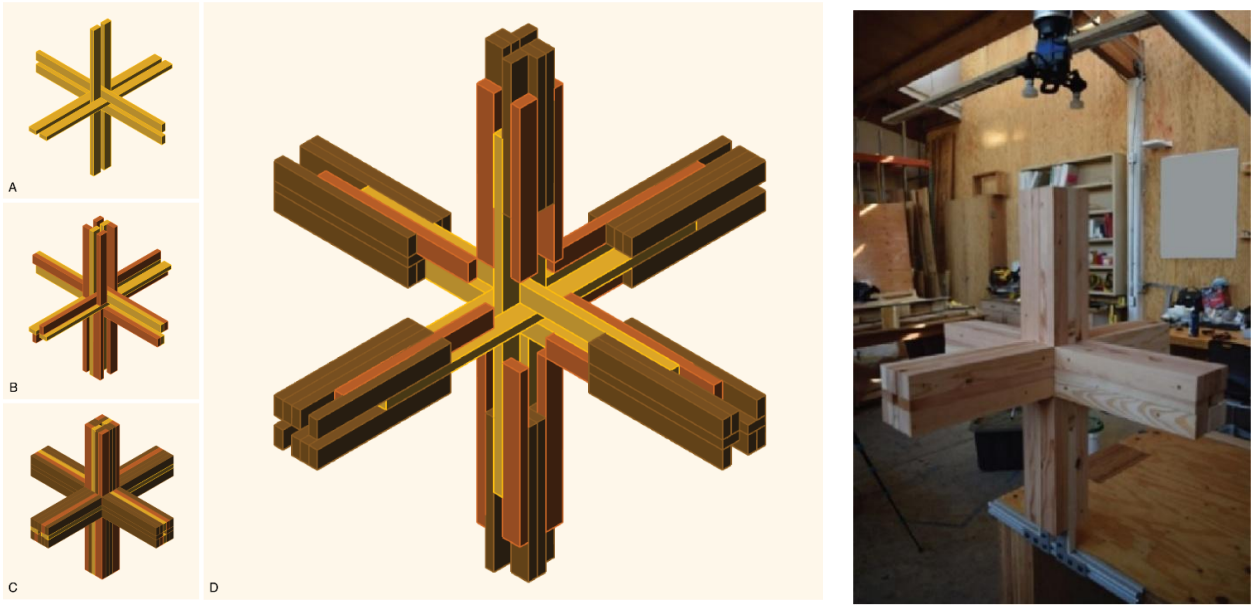


Figure 22. Left: Build order and exploded axon of the 3D joint. The colors represent component length. A: Yellow, 36". B: Orange, 17.5". C: Brown, 15.5". On the right is the completed three-dimensional multi-axis joint, viewed from above under the UR20 after final assembly.

Part 2 extends this additive assembly approach into three dimensions. The completed joint totals sixty-six discrete members: six primary pieces, four at thirty-six inches and two at thirty-nine inches, form the reciprocal core where all three orthogonal axes meet; sixteen seventeen-and-a-half-inch members build outward as a secondary layer; and forty-four fifteen-and-a-half-inch members close out the assembly, locking the longer spanning pieces in place. As with the planar joint in Part 1, every member shares a single two-inch by one-inch cross section, so the same pickup geometry could be reused across all sixty-six pieces, with only each board's length and final placement changing from one piece to the next.

Because the joint is symmetric about its center along each of its three axes, roughly half of the placements did not need to be programmed individually. After scripting and testing the geometry-derived pickup-and-placement sequence for one side of an axis, the physical mounting bracket holding the robot's base plate to the table was unbolted, rotated one hundred eighty degrees, and reattached, allowing the same program to build the opposing side without any changes to the code. The six central members, which sit at the joint's core and have no mirrored counterpart, were the only pieces programmed individually outside this pairing. This approach, developed after the robot began struggling to reach placements on the far side of the joint, particularly the lower members,

meaningfully reduced the scripting burden of a joint an order of magnitude larger than Part 1's planar connection.

The joint's geometry was also directly shaped by the robot's physical working envelope. Two of the six primary members were lengthened during fabrication from the original thirty-six-inch design dimension to thirty-nine inches, adding three inches of clearance between the placement plane and the worktable so the arm could complete each placement motion without striking the table surface. As in Part 1, where the UR20's reach and payload limits set the practical bounds on piece size, this adjustment reinforces that the robotic assembly process was not simply a delivery mechanism for a fixed design, but an active constraint that shaped the joint's final form.

Part 2's much larger, mirrored, multi-board program surfaced failure types that never appeared in Part 1. Boards that ran correctly on their own began faulting only once merged into the full sequence, because each board after the first inherited the prior board's ending arm configuration at their shared home position instead of resolving a fresh one, a problem invisible until the joint reached its full scale. Precise calibration of the gripper's true reach and mass also mattered more at this scale, where small errors compound across sixty-six placements rather than the more forgiving margins of Part 1's larger, fewer-piece layers.



Figure 23. Build sequence of the first layer of the multi-axis joint and the start of the second. Read from left to right, top to bottom.

5.5 Design Concept

These structural advantages point toward a broader application worth showing: the same rigid-arm logic that resists moment locally could extend directly into the beam itself as part of one continuous robotically assembled member, rather than stopping at a single joint. Early concept renders illustrate this, showing the cruciform joint's core tapering outward along one arm into a full beam section, built up from the same discrete, additively placed members rather than transitioning to a separately milled beam. Nothing at this scale has been fabricated or tested structurally, but the concept demonstrates, in the same spirit as the real-world use-case renders in 5.2, that the density-and-overlap logic developed in Part 1 could extend beyond an isolated connection into an actual structural element within a building.

The three-dimensional joint's design-concept potential is broader still, precisely because its reciprocal-frame logic already resolves force along three axes rather than two. Where the planar joint's beam-integration concept extends a single arm outward into a continuous member, the completed 3D joint suggests a more general building block: a fully three-dimensional node, now built and tested at prototype scale, that could anchor an entire structural grid rather than a single beam line, using the same additively placed, fiber-aligned members developed for the prototype. Early conceptual applications illustrate this range. An interior moment-resisting grid could repeat the joint at every column-beam-beam intersection of a multi-bay floor plate, carrying the same continuity advantage described in section 5.3 across two spanning directions simultaneously rather than one. A branching, tree-like column could extend the joint's reciprocal geometry upward from a single base into multiple diverging members, distributing load the way the joint itself already distributes it among its sixty-six pieces. And because the joint's arms can be sized and angled independently, the same core geometry could scale down into a lighter, span-oriented connection for a truss or bridge-type structure, or scale up into a heavier ground-bearing column base. Together, these joints indicate that the 3D joint's value extends past the single connection tested here, toward a genuinely three-dimensional structural vocabulary that the planar joint's two-axis logic could not offer on its own.

This same reciprocal-frame potential is reflected in the 3D joint's material composition, developed in coordination with the project's structural committee input introduced in Chapter 4. Figure 24 shows this directly: the design concentrates continuous, higher-grade members along the joint's outer arms, precisely where the joint's chords carry the greatest combined tension and

compression, and reserves shorter, less continuous, lower-grade members, including an interior layer running between the exterior primary members, for the joint's low-stress interior core. Figure 25 makes the underlying force logic explicit: within each beam-like chord passing through the joint, the top members carry tension and the bottom members carry compression, consistent with standard moment-resisting beam behavior, while every column member passing through the joint's center remains in axial compression throughout. Read together, these two figures support treating a greater degree of member interconnection, longer, more continuous pieces spanning farther across the joint, as most valuable near the joint's outer edges rather than its geometric center, since that is where the joint's actual internal forces peak.

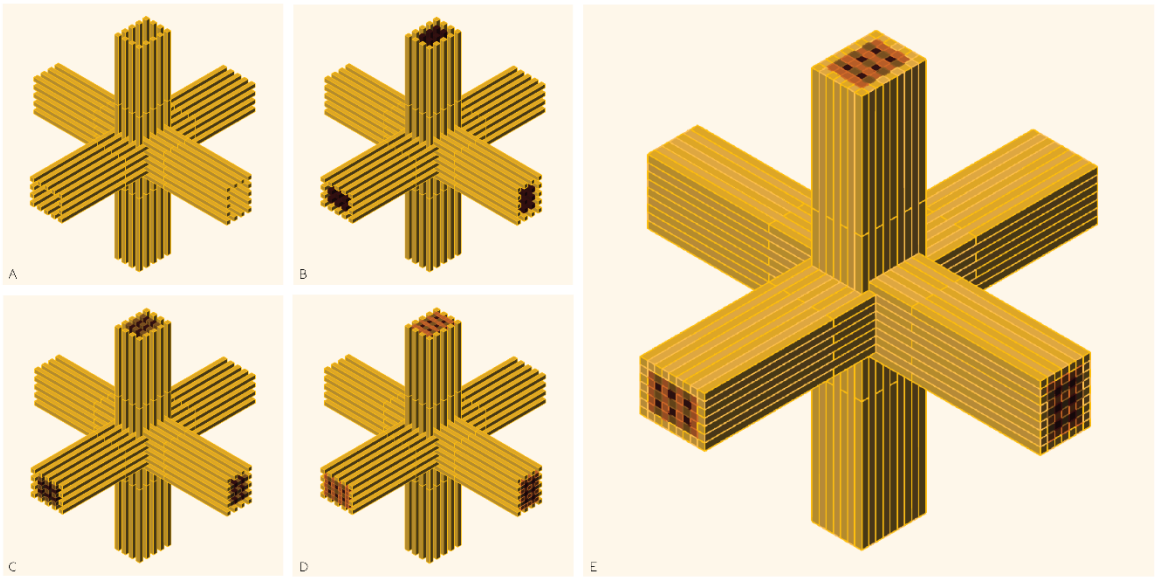


Figure 24. Material-grade distribution for the three-dimensional multi-axis joint. Yellow members are the higher-grade, primary exterior material; all other members are lower-grade infill, including an interior layer running between the exterior primary members. A: Baseline case, built entirely from higher-grade material. B–D: Infill progressively introduced at the joint's lower-stress locations, while higher-grade material remains continuous along the outer, moment-resisting arms. E: Larger view of the completed joint, showing the full assembly and material distribution in detail.

This joint-level logic extends directly to the system scale. Figure 26 shows the three-dimensional multi-axis joint's partial-column condition repeated across a larger structural grid, each node built from the same reciprocal geometry but requiring only a partial column length rather than a single continuous member running the building's full height. The same higher-grade, more continuous material used at each joint's outer arms carries directly into the columns and beams framing into it, while lower-grade, less continuous material remains reserved for each node's low-stress core, the same grading logic shown in Figure 24 repeated at every intersection of the grid. At the system scale, each node can be built one of two ways: as an integrated connector, formed as a single continuous unit with the column running through it, or as a standalone connector, a separate joint attached to the column rather than continuous with it. Lining every node at a given story up as the same type would create a continuous plane of standalone connections running through the entire structure at that elevation, concentrating a potential structural weak point across every bay at once rather than isolating it to a single connection. Staggering integrated and standalone connectors across the grid, alternating both along each column and across each story, avoids that condition: at any given elevation, enough columns remain continuous through that point to help redistribute load around the standalone connections nearby, the same logic behind staggered rebar splices in concrete and running-bond coursing in masonry. As with the other applications introduced above, this system-scale arrangement has not been modeled structurally or fabricated at building scale, but it

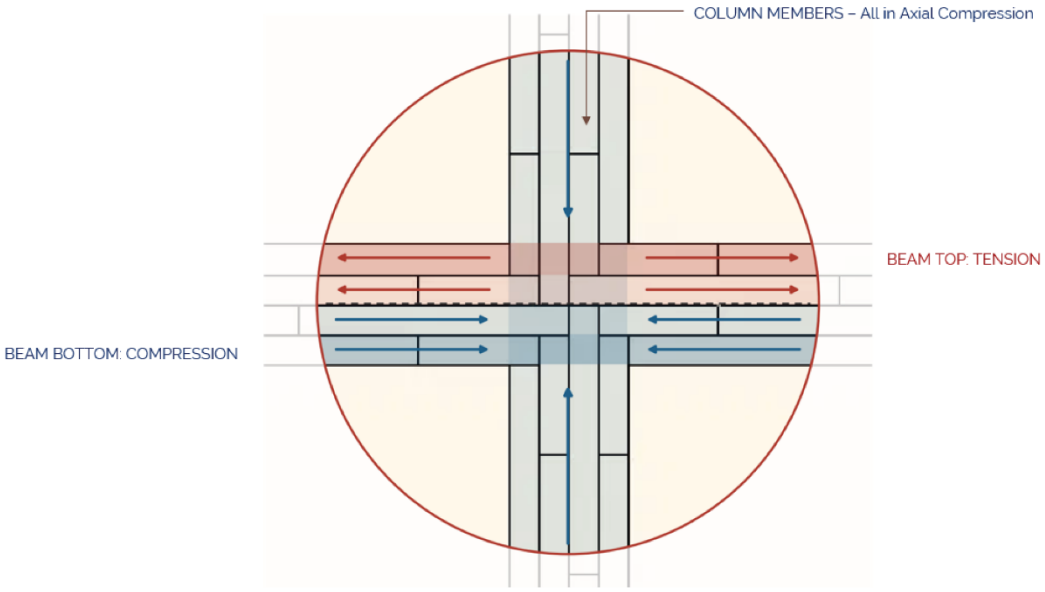


Figure 25. Force distribution diagram for the 3D joint's beam-column intersection. Column members passing through the joint remain in axial compression throughout; within each beam chord, the top members carry tension and the bottom members carry compression, consistent with typical moment-resisting beam behavior at a rigid joint.

demonstrates how the joint's internal material logic, and its connector type, could compose into a full structural system rather than remain confined to a single connection. Figure 27 extends this same joint logic to a reciprocal frame arrangement rather than an orthogonal grid, offsetting each beam's bearing point onto its neighbor's arm instead of a shared column, as the build sequence in the figure shows step by step. The same rigid-arm argument developed in 5.3 still applies at this larger scale: because the joint's arms move each beam's effective moment demand outward, the beam itself needs less material to resist it, whichever arrangement organizes the bay. At the system scale, that reduction repeats at every bay, implying a meaningful reduction in the overall fiber required across a full structure, though quantifying that reduction in material or cost terms is left as future work rather than claimed here.

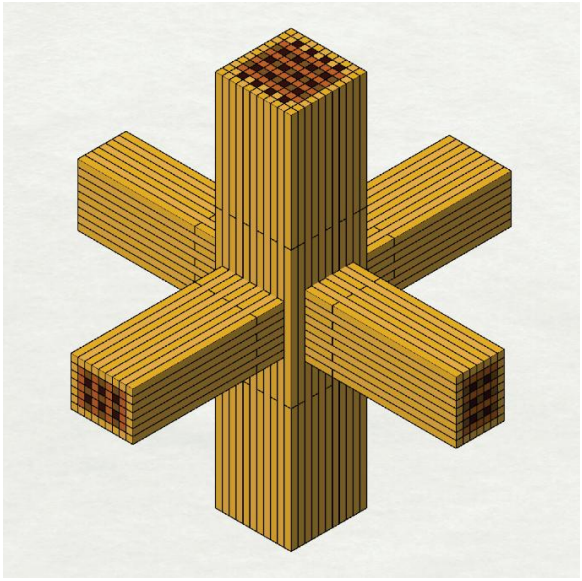


Figure 26. Cross-sectional proportioning at the three-dimensional multi-axis joint, informed by the force distribution shown in Figure 25. The column, carrying only axial compression, is sized as a large, square section with no preferred bending direction. Each beam arm, carrying the tension and compression chords described above, is sized deeper than it is wide, the standard timber beam proportion for resisting bending.

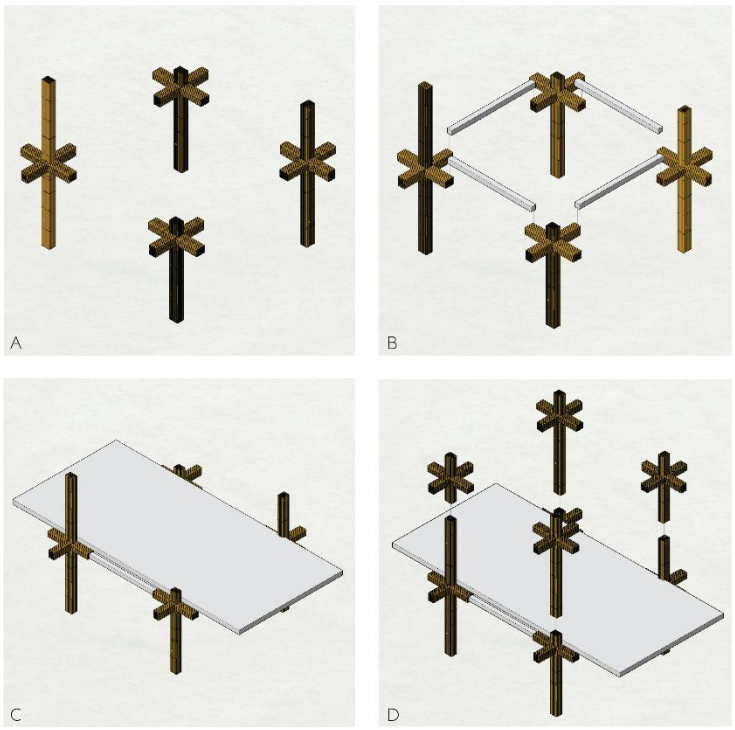


Figure 27. Build sequence for a reciprocal frame of four joints. Four joints that carry a continuous column through them are placed, spliced at different lengths, forming an offset that defines the reciprocal frame (A). Beams connect opposite joints arm-to-arm rather than meeting at a shared column (B). A floor panel seats onto the beams (C). The remaining joint and beam close the loop under that same panel (D).

CHAPTER VI
DISCUSSION

6.1 Fabrication Performance Across Both Prototypes

Across both builds, the fabrication process surfaced two distinct categories of challenge: software and data-alignment issues within the parametric scripting, most evident in Part 1, and physical calibration issues on the robot itself, which became more pronounced as Part 2 scaled up. Unlike the hand-milling tolerance limitation described in Chapter 4, every difficulty in these two categories was fully diagnosable and solvable once isolated, and none prevented successful assembly of either joint. Part 1's problems, detailed in Section 5.2, traced almost entirely to misaligned or misindexed data rather than any hardware fault; Part 2's, detailed in Section 5.4, stemmed instead from errors that only appeared once individually working boards were merged into the full sixty-six-piece sequence, where small calibration errors could compound across far more placements than Part 1 required. That progression, from data-logic errors to scale-compounding ones, tracks the added complexity of the second build rather than any decline in fabrication reliability: each issue had an identified and implemented fix, distinguishing both builds clearly from the fabrication-precision limitation discussed in Chapter 4, where cumulative hand-milling tolerance, not the robot or its script, remained the primary source of uncertainty in the finished joints.

CHAPTER VII
CONCLUSION

7.1 Summary

This thesis set out to test the idea that a timber joint's fiber orientation does not have to be inherited from whatever a single length of sawn stock happens to provide, or from what a milling tool leaves behind, but can instead become a design decision made as the joint is built. Where conventional subtractive joinery cuts a connection out of a finished member, the additive approach developed here builds a connection up from many small, individually placed wood elements, robotically assembled so that each piece's orientation, position, and material can be chosen deliberately. This required extending robotic fabrication in timber construction beyond its typical role automating machining, into a role assembling many discrete parts into a single composite connection.

Two joint typologies were designed and robotically fabricated to test this approach: a five-layer, 104-piece clad planar joint that distributes load across many contact points rather than a single hierarchical connection, and a three-dimensional, sixty-six-piece reciprocal joint that extends the same additive logic across three orthogonal axes. Both were completed using a UR20 robotic arm and a parametric, code-driven assembly workflow developed specifically for this project, one that grew markedly more capable across the two builds, from manually triggered pickup sequences in early proof-of-concept work to fully scripted grip, release, speed, and precision control by the second joint.

Building both joints surfaced two distinct kinds of fabrication challenge. Software and robot-calibration issues, misaligned data streams, gripper timing, joint-limit faults at larger scales, proved fully diagnosable and solvable once properly isolated, and never limited what either joint could achieve. The more persistent limiting factor was upstream of the robot entirely: cumulative imprecision from milling the individual wood elements by hand, which a more automated or more skilled fabrication process would likely resolve.

A structural comparison against the Heartwood building, a real all-wood precedent, suggested two potential advantages of the additive approach: a moment-resisting connection behavior that could reduce material demand in the adjoining beam, and a fire-continuity advantage from avoiding the aligned fabrication gaps that a subtractive, notched connection creates. Both arguments follow

standard structural reasoning applied to the joint's geometry, but neither has been confirmed through physical load testing or fabrication of the specific comparison case, and both are identified explicitly as future work rather than demonstrated results.

Taken together, this work demonstrates that fiber-aligned, additively assembled timber joints are structurally reasoned and physically buildable at prototype scale, and it develops a real, repeatable robotic methodology for constructing them. What remains open, addressed in the following section, is the empirical validation, quantified strength-to-mass performance, comparative load testing, and structural confirmation of the arguments made here, that would be needed to fully answer the research questions posed in Chapter 1.

7.2 Limitations and Future Work

A third joint typology, a robotically assembled angled joint, was scoped early in the project as a conceptual extension of the reciprocal joint system but was not pursued due to time constraints within this thesis. It remains a promising direction for future work, extending the additive assembly logic developed for the planar and reciprocal joints to non-orthogonal, angled configurations.

Fabrication precision is also identified as a direction for future work. Because the discrete elements used in this thesis were milled by hand, minor cumulative tolerance errors and inconsistencies between pieces were introduced that a more automated or more skilled fabrication process would likely avoid. Producing these elements with a CNC mill or laser cutter, where joint geometry allows, or through the work of a more experienced craftsperson, is expected to improve both consistency and assembly speed beyond what was achieved in this thesis.

Material stratification is also identified as a direction for future work. The built prototypes in this thesis each used a single wood species, since testing the structural contribution of a multi-species scheme was beyond what could be verified without load testing. That stratification logic, assigning stronger species to zones of concentrated compressive or tensile demand and weaker or offcut species to lower-demand infill, remains a design consideration worth pursuing: it would let a joint's internal material composition be tuned by function and adapted regionally to locally available hard and softwoods and by application. Testing this logic under structural load is a necessary next step to validate it beyond the design stage.

The rigid-end-zone idealization used to describe the planar joint's moment-resisting behavior in Chapter 5 is also identified as a direction for future work. That idealization assumes the joint's arms are stiff enough relative to the beam to be treated as a non-bending end zone, an assumption that

has not yet been checked against the joint's actual built dimensions and species stiffness. Confirming the real arm-to-beam stiffness ratio, and eventually load testing the assembled connection directly, would be necessary before the reduced-moment behavior described here could be treated as more than an illustrative structural argument.

Fixation method is also identified as a direction for future work. The two prototypes built for this thesis were joined using screws and glue rather than an entirely mechanical, wood-only connection, a practical choice driven by the fabrication tools and facility access available for this project rather than a limitation of the additive assembly approach itself. Wood dowel connections are a strong candidate for closing that gap: because each joint is already built from many individually placed members, inserting dowels through aligned bore holes at the interfaces between pieces extends the same robotic placement logic already developed here rather than requiring a different fabrication process. Doing so would remove the adhesive and metal-fastener dependencies discussed in Chapter 2, directly addressing the recyclability, off-gassing, and fire-vulnerability concerns those methods carry, while keeping both assembly and disassembly fully mechanical.

A tension worth naming directly is between designing a joint's fiber alignment for one specific, well-understood load case and preserving the general-purpose adaptability a conventional, uniformly milled connection offers almost by default: because this approach chooses each member's position, orientation, and grade for a particular structural demand, that same specificity could make it less forgiving of load conditions that differ meaningfully from the one it was designed around. A parametrically driven fiber-alignment strategy that responds to a defined range of load cases, rather than a single idealized one, is a necessary next step before this approach could be applied confidently to real, variably loaded structures.

Extending this additive logic beyond the connection itself is also identified as a direction for future work. The same principle, placing many small, individually oriented wood elements according to structural demand rather than accepting a single member's inherited properties, applies just as naturally to panels as it does to point connections, and could extend further to hybrid assemblies that combine additively built panels with additively built connectors into one continuously reasoned structural system.

7.3 Impact

The most direct impact of this work is methodological: it demonstrates that robotic fabrication in timber construction does not have to remain limited to automating what a mill already does,

cutting and drilling faster and more precisely, but can instead build a joint's structural logic directly, piece by piece, as the connection itself is formed. This reframing addresses the gap identified in Chapter 2, where connection manufacturing has stayed separated from member manufacturing even as digital fabrication tools have grown more capable. The two joints developed here, and the fabrication methodology built to produce them, offer other researchers and practitioners a concrete, tested starting point for pursuing additive timber joinery further, rather than a purely theoretical proposal.

This approach also carries real material and environmental implications. Because additive joints rely on wood-to-wood contact rather than steel plates, bolts, or dowels, moving toward this kind of joinery reduces the embodied carbon tied to metal fastener production entirely. Aligning fiber with anticipated force paths, rather than accepting whatever orientation sawn stock provides, allows narrower members to do the same structural work, lowering material demand at the scale of an entire structure rather than a single connection. The same logic extends to species selection: because each element in an additive joint is placed individually, lower-grade material or offcuts that would otherwise go to waste could be used deliberately in lower-demand zones of a joint, a possibility this thesis identifies as a design consideration rather than a demonstrated result, but one with genuine material-efficiency implications worth pursuing.

Beyond the joint itself, this work points toward a different way of thinking about mass timber structure generally. The real-world use-case renders developed for the planar joint, and the beam-integration concept introduced in Chapter 5, both show that additive joinery need not stay confined to an isolated connection sample. The same logic can extend into a full structural grid or a continuously built beam, giving architects and engineers a design vocabulary that treats the joint and the member as part of one continuous, deliberately formed material system rather than two separately manufactured parts joined after the fact. That shift matters specifically for an architecture program's stake in this work, connecting a manufacturing-process investigation to a genuine question of building form.

Finally, this work speaks to a known problem in subtractive, notched timber connections: the small fabrication gaps inherent to a resting, milled interface align into a continuous vertical path, and current practice treats that path as something to seal after the fact, using intumescent tape at each floor line, rather than something to design out of the connection itself. The planar joint's arm geometry offers a more elegant alternative: the same outward shift that reduces bending moment in the adjoining beam also removes the resting interface that creates that aligned gap in the first place,

addressing a fire-safety liability and a structural inefficiency with a single geometric move rather than two separate fixes. This reframes joint geometry itself as a life-safety consideration, not only a structural or material-efficiency one, but also as a case this thesis makes at the design level.

REFERENCES CITED

[1] Dissanayake, Harshani, Tharaka Gunawardena, and Priyan Mendis. "Adaptation of Connection Systems for Integration with Engineered Wood Products in Buildings: A Systematic Review." Buildings 15, no. 7 (2025): 1131. https://doi.org/10.3390/buildings15071131.

[2] Slater, Duncan, and Roland Ennos. "Interlocking Wood Grain Patterns Provide Improved Wood Strength Properties in Forks of Hazel (Corylus avellana L.)." Arboricultural Journal 37, no. 1 (2015): 21–32. https://doi.org/10.1080/03071375.2015.1012876.

[3] Kunic, Anja, Roberto Naboni, Aljaz Kramberger, and Christian Schlette. "Design and Assembly Automation of the Robotic Reversible Timber Beam." Automation in Construction 123 (March 2021): 103531. https://doi.org/10.1016/j.autcon.2020.103531.

[4] Jesús de-los-Aires-Solís, Antonio, and Francisco Gonzalez-Quintial. "A Wood-Wood Joining System Suitable for Digital Fabrication and Its Application in the Design of a 'Wood-Only' Spatial Module." Frontiers of Architectural Research 12, no. 3 (2023): 523–40. https://doi.org/10.1016/j.foar.2022.12.005.

[5] Apolinarska, Aleksandra Anna, Matteo Pacher, Hui Li, et al. "Robotic Assembly of Timber Joints Using Reinforcement Learning." Automation in Construction 125 (May 2021): 103569. https://doi.org/10.1016/j.autcon.2021.103569.

[6] Kanasaki, Kenji, and Hiroya Tanaka. "Traditional Wood Joint System in Digital Fabrication." In eCAADe 31, 711–717. 2013. https://doi.org/10.52842/conf.ecaade.2013.1.711.

[7] Zhao, Jiangyang, Asterios Agkathidis, Davide Lombardi, and Hanmei Chen. "Reinterpreting the Dougong Joint: A Systematic Review of Robotic Technologies for the Assembly of Timber Joinery." Architectural Science Review 68, no. 1 (2025): 65–79. https://doi.org/10.1080/00038628.2024.2339995.

[8] Grič, Michal, Pavol Joščák, Ilkka Tarvainen, et al. "Mechanical Properties of Furniture Self-Locking Frame Joints." BioResources 12, no. 3 (2017): 5525–38. https://doi.org/10.15376/biores.12.3.5525-5538.

[9] Han, Lei, Andreja Kutnar, Jakub Sandak, Iztok Šušteršič, and Dick Sandberg. "Adhesive- and Metal-Free Assembly Techniques for Prefabricated Multi-Layer Engineered Wood Products: A Review on Wooden Connectors." Forests 14, no. 2 (2023): 311. https://doi.org/10.3390/f14020311.

[10] Gamerro, Julien, Jean Francois Bocquet, and Yves Weinand. "Experimental Investigations on the Load-Carrying Capacity of Digitally Produced Wood-Wood Connections." Engineering Structures 213 (June 2020): 110576. https://doi.org/10.1016/j.engstruct.2020.110576.

[11] Gamerro, Julien, Jean Bocquet, and Yves Weinand. "A Calculation Method for Interconnected Timber Elements Using Wood-Wood Connections." Buildings 10, no. 3 (2020): 61. https://doi.org/10.3390/buildings10030061.

[12] Fang, Demi. Timber Joinery in Modern Construction: Mechanical Behavior of Wood-Wood Connections. N.d.

[13] Fang, Demi, and Caitlin Mueller. "Mortise-and-Tenon Joinery for Modern Timber Construction: Quantifying the Embodied Carbon of an Alternative Structural Connection." Architecture, Structures and Construction 3, no. 1 (2023): 11–24. https://doi.org/10.1007/s44150-021-00018-5.

[14] Abed, Joseph, Scott Rayburg, John Rodwell, and Melissa Neave. "A Review of the Performance and Benefits of Mass Timber as an Alternative to Concrete and Steel for Improving the Sustainability of Structures." Sustainability 14, no. 9 (2022): 5570. https://doi.org/10.3390/su14095570.

[15] Ijeoma, Muzan Williams, Sovanroth Ou, Great William Ijeoma, Michael Stoner, Brandon Ross, Weichiang Pang, Patricia Layton, Dustin Albright, Hao Chen, Amin Nabati, and Michael Carbajales-Dale. "Assessing the Energy Demand, Carbon Footprint and Other Environmental Impacts from Mass Timber Production: A Critical Review and Meta-Analysis." Environmental Research Communications 7 (2025): 112001.

[16] Willmann, Jan, Michael Knauss, Tobias Bonwetsch, Anna Aleksandra Apolinarska, Fabio Gramazio, and Matthias Kohler. "Robotic Timber Construction — Expanding Additive Fabrication to New Dimensions." Automation in Construction 61 (2016): 16–23. https://doi.org/10.1016/j.autcon.2015.09.011.

[17] Raspall, Felix, Maximiliano Pazols, Ulises Campodonico, Agustín Hurtado, and Nicolás Pereda. Development of a Wood Frame Structure with 3D Printed Clip Joints: A Design Studio Exploration. n.d. https://papers.cumincad.org/data/works/att/sigradi2024_336.pdf.

[18] Kramberger, Aljaz, Anja Kunic, Iñigo Iturrate, Christoffer Sloth, Roberto Naboni, and Christian Schlette. "Robotic Assembly of Timber Structures in a Human-Robot Collaboration Setup." Frontiers in Robotics and AI 8 (2022): 768038. https://doi.org/10.3389/frobt.2021.768038.

[19] Nguyen, Anh Chi, Petras Vestartas, and Yves Weinand. "Design Framework for the Structural Analysis of Free-Form Timber Plate Structures Using Wood-Wood Connections." Automation in Construction 107 (November 2019): 102948. https://doi.org/10.1016/j.autcon.2019.102948.

[20] StructureCraft. "Philip J. Currie Dinosaur Museum | Timber Design." Accessed November 21, 2025. https://structurecraft.com/projects/philip-j-currie-dinosaur-museum.

[21] Shigeru Ban Architects. "Tamedia New Office Building." Accessed November 21, 2025. https://shigerubanarchitects.com/works/cultural/tamedia-new-office-building/.

[22] Atelierjones. "Heartwood." Accessed November 21, 2025. https://www.atelierjones.com/heartwood.

[23] Whitehead, Jaimie, Hamish Strange, and Nicki Vance. "Design of a Timber Diagrid Seismic Structural System." World Conference on Timber Engineering 2025, 5279–88. https://doi.org/10.52202/080513-0649.

[24] Porras, Emerson, Doris Esenarro, Lidia Chang, Walter Morales, Carlos Vargas, and Joseph Sucasaca. "Toward Cost-Effective Timber Shell Structures through the Integration of Computational Design, Digital Fabrication, and Mechanical Integral 'Half-Lap' Joints." Buildings 14, no. 6 (2024): 1735. https://doi.org/10.3390/buildings14061735.

[25] Armitage-Hookes, Flo. "Why dRMM's New Knuckle Joints Using Homegrown Hardwood Are Game-Changing for Engineered Timber." RIBAJ, December 11, 2025. https://www.ribaj.com/intelligence/drmm-clt-research-knuckle-joint/.

[26] Mehra, Sameer, Conan O'Ceallaigh, Adeayo Sotayo, Zhongwei Guan, and Annette M. Harte. "Experimental Investigation of the Moment-Rotation Behaviour of Beam-Column Connections Produced Using Compressed Wood Connectors." Construction and Building Materials 331 (May 2022): 127327. https://doi.org/10.1016/j.conbuildmat.2022.127327.

[27] Pastrana, Rafael, and Zhao Ma. "Computing Rebar Layouts Aligned with the Principal Stress Directions: A Distance-Constrained Tracing Approach." ACADIA 2023: Habits of the Anthropocene, 140–52.

[28] Amtsberg, Felix, and Felix Raspall. "Bamboo³." In Learning, Adapting and Prototyping: Proceedings of the 23rd International Conference of the Association for Computer-Aided Architectural Design Research in Asia (CAADRIA) 2018, Volume 1, edited by T. Fukuda, W. Huang, P. Janssen, K. Crolla, and S. Alhadidi, 245–254. Hong Kong: CAADRIA, 2018. https://papers.cumincad.org/data/works/att/caadria2018_304.pdf

[29] TRIQBRIQ AG. "TRIQBRIQ System." Accessed August 27, 2026. https://triqbriq.de/en/triqbriq-system/.

[30] Thoma, Andreas, Arash Adel, Matthias Helmreich, Thomas Wehrle, Fabio Gramazio, and Matthias Kohler. "Robotic Fabrication of Bespoke Timber Frame Modules." In Robotic Fabrication in Architecture, Art and Design 2018, edited by Jan Willmann, Philippe Block, Marco Hutter, Kendra Byrne, and Tim Schork, 447–458. Cham: Springer, 2019. https://doi.org/10.1007/978-3-319-92294-2_34.